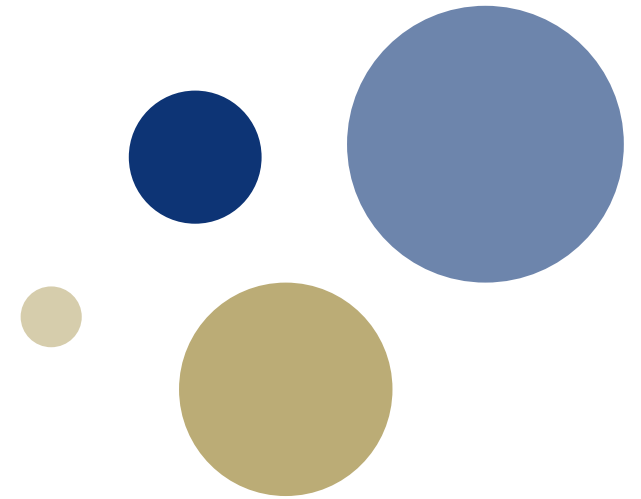




Norwegian University of
Science and Technology



The high-energy Galactic gamma-ray emission: the diffuse component and the role of unresolved pulsar wind nebulae

Presented by: Vittoria Vecchiotti

Based on work done in collaboration with: F. L. Villante, G. Pagliaroli, and M. Cataldo

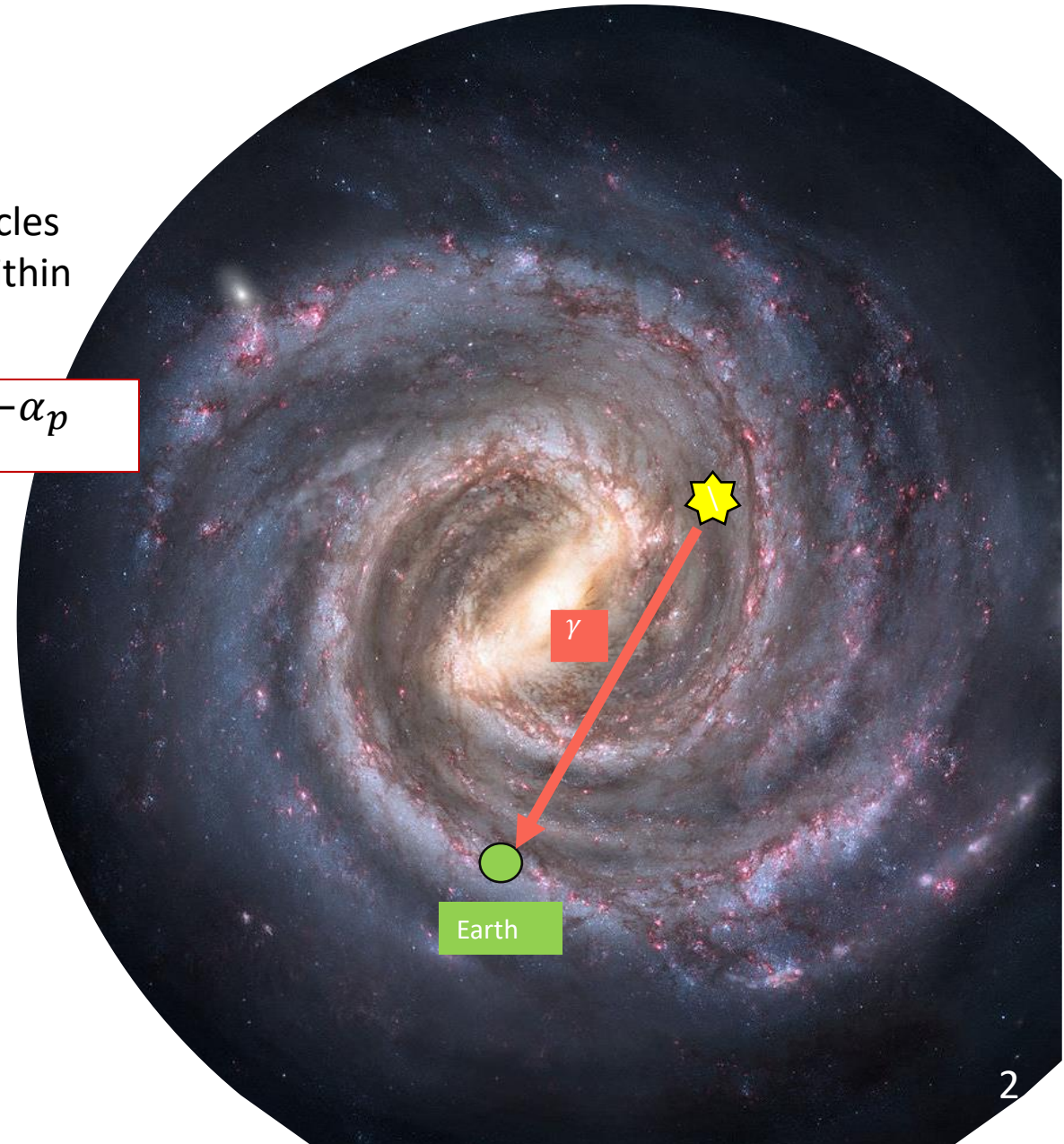
Total Galactic emission above GeV:

$$\phi_{\gamma,tot} = \phi_{\gamma,s} + \phi_{\gamma,diff}$$

Source component is due to the interaction of accelerated particles (hadrons or leptons) with the ambient medium (ISM or CMB) within or close to an acceleration site (such as PWNe, SNRs);

Injected spectrum at the source location:

$$\varphi_{p,s}(E) \sim E^{-\alpha_p}$$



Total Galactic emission above GeV:

$$\phi_{\gamma,tot} = \phi_{\gamma,s} + \phi_{\gamma,diff}$$

Source component is due to the interaction of accelerated particles (hadrons or leptons) with the ambient medium (ISM or CMB) within or close to an acceleration site (such as PWNe, SNRs);

Injected spectrum at the source location:

$$\varphi_{p,s}(E) \sim E^{-\alpha_p}$$

Gamma-ray spectrum at the source location:

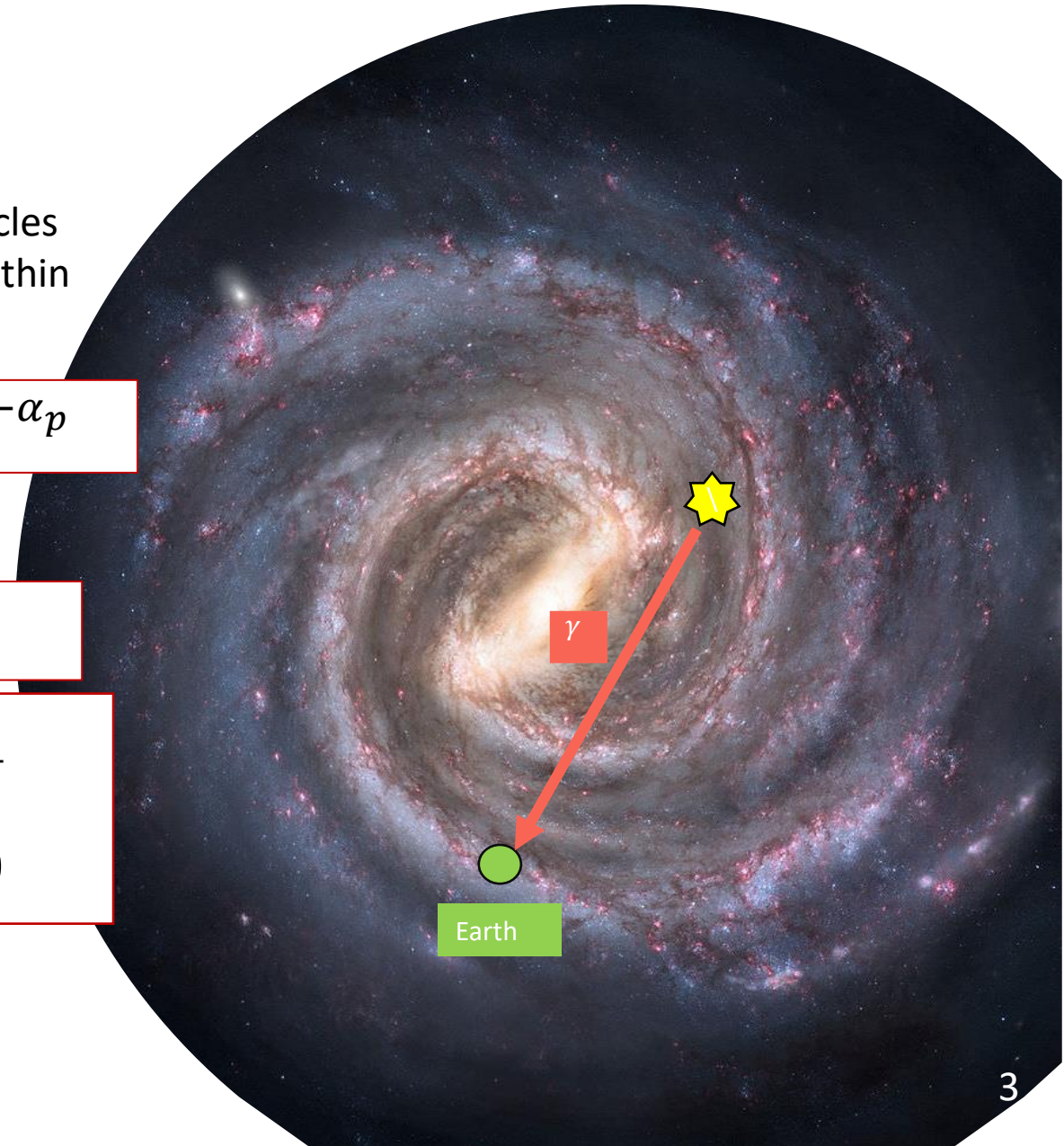
• (hadrons) pp interaction:

$$\varphi_{\gamma,s}(E) \sim E^{-(\alpha_p-0.1)}$$

• (leptons) Inverse Compton:

$$\varphi_{\gamma,s}(E) \sim \begin{cases} E^{-\frac{(\alpha_p+1)}{2}} \\ E^{-(\alpha_p+1)} \end{cases}$$

It coincides with the one measured on Earth (*gamma rays propagate along straight lines and, on Galactic scales, the absorption is negligible*).



Total Galactic emission above GeV:

$$\phi_{\gamma,tot} = \phi_{\gamma,s} + \phi_{\gamma,diff}$$

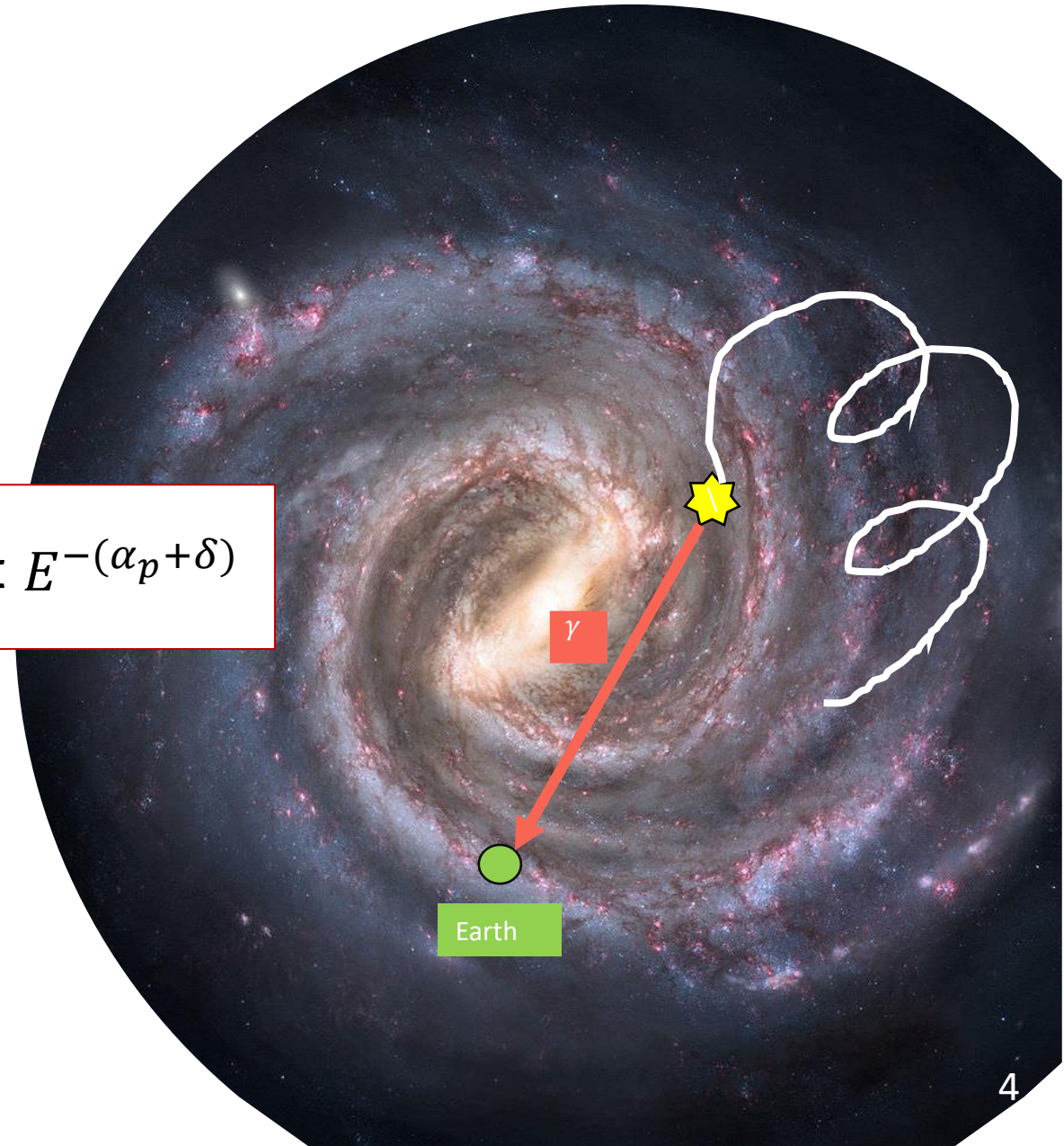
Accelerated hadrons can escape the source and propagate in the Galaxy. They girates along the Galactic magnetic field lines and are scattered by magnetic field turbulence.

The diffusion coefficient:

$$D(E) \propto E^\delta$$

The CR spectrum after propagation:

$$\varphi_p(E) \propto \frac{\varphi_{p,s}(E)}{D(E)} \propto E^{-(\alpha_p+\delta)}$$



Total Galactic emission above GeV:

$$\phi_{\gamma,tot} = \phi_{\gamma,s} + \phi_{\gamma,diff}$$

Accelerated hadrons can escape the source and propagate in the Galaxy. They girates along the Galactic magnetic field lines and are scattered by magnetic field turbulence.

The diffusion coefficient:

$$D(E) \propto E^\delta$$

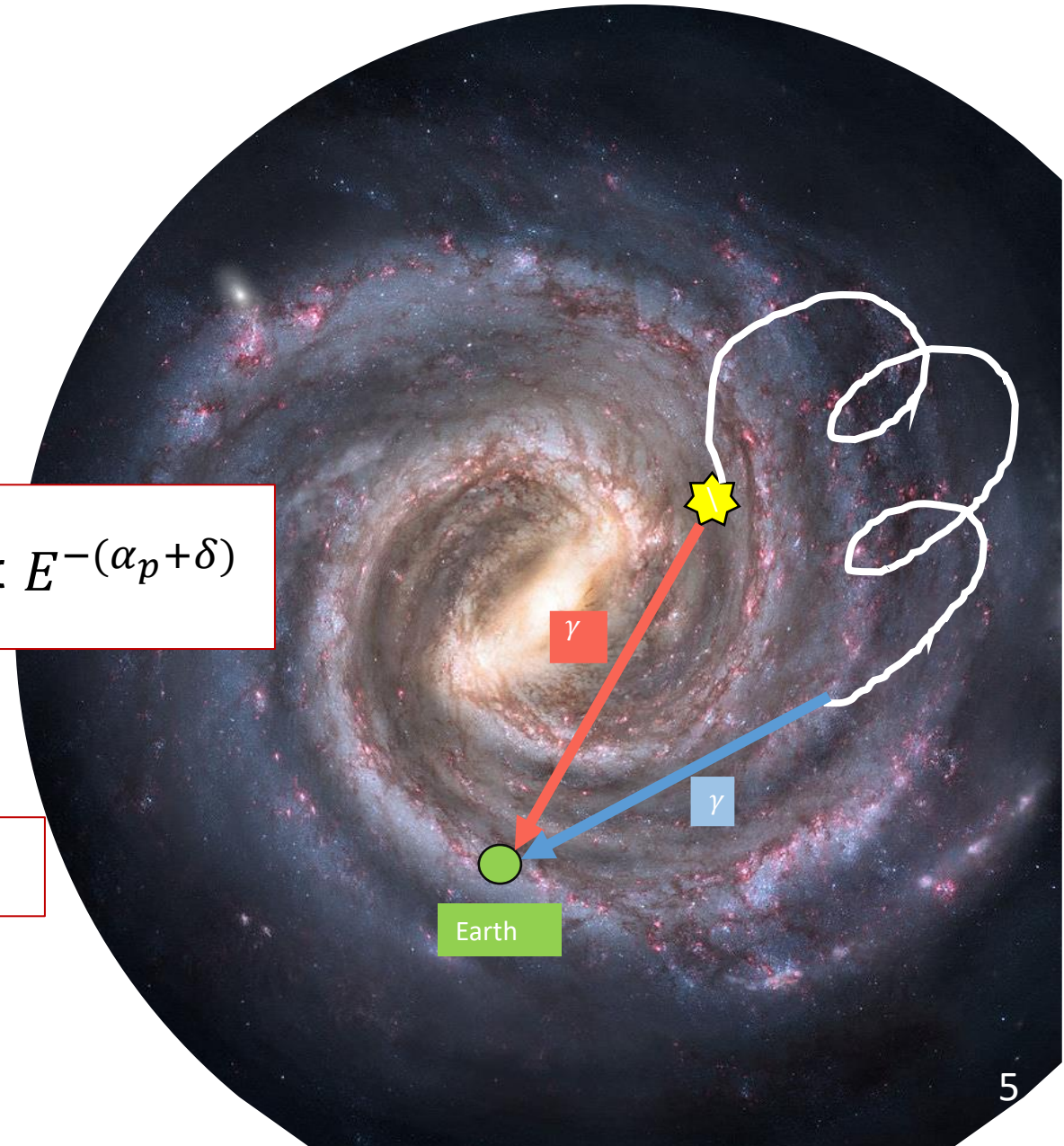
The CR spectrum after propagation:

$$\varphi_p(E) \propto \frac{\varphi_{p,s}(E)}{D(E)} \propto E^{-(\alpha_p+\delta)}$$

Diffuse component is due to the interaction of cosmic rays with the interstellar medium;

Gamma-ray spectrum:

$$\varphi_{\gamma,diff}(E) \propto E^{-(\alpha_p+\delta-0.1)}$$



Total Galactic emission above GeV:

<https://fermi.gsfc.nasa.gov/ssc/observations/types/allsky/>

$$\phi_{\gamma,tot} = \phi_{\gamma,s} + \phi_{\gamma,diff}$$

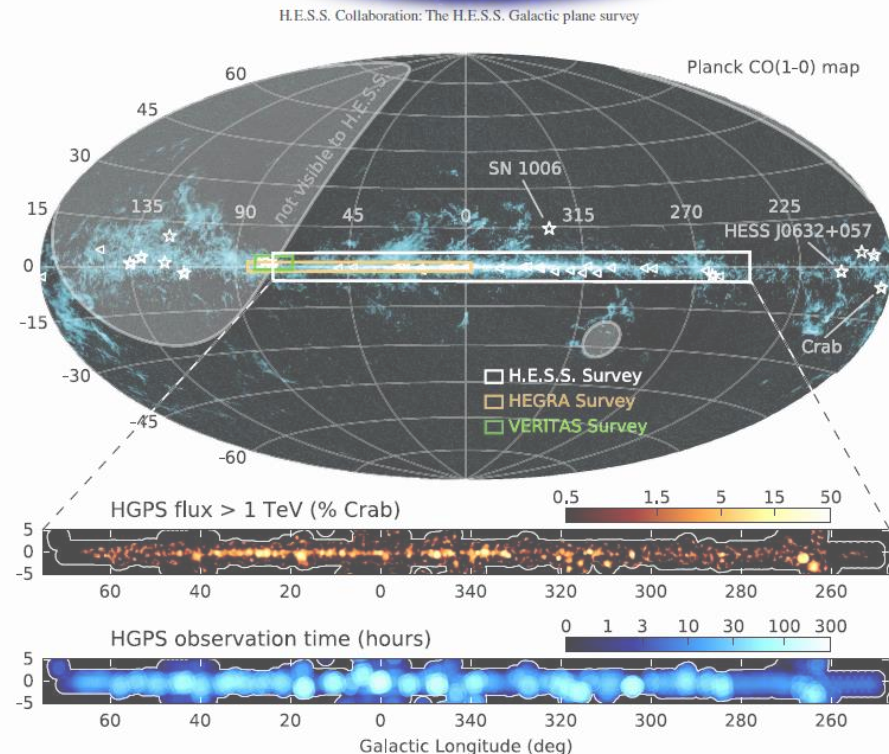
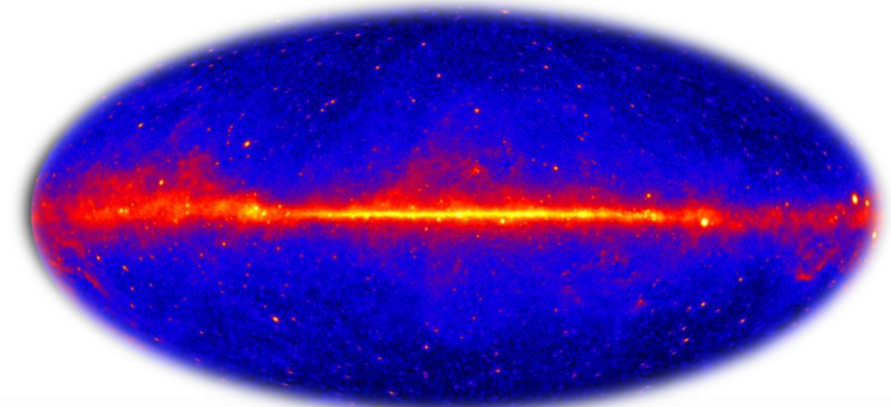
The relative importance of the above terms changes accordingly to the considered energy range:

- GeV energy: $\phi_{\gamma,diff} > \phi_{\gamma,s}$
- TeV energy: $\phi_{\gamma,diff} \simeq \phi_{\gamma,s}$

This behavior is due to the fact that sources have harder spectrum than the diffuse emission.

$$\phi_{\gamma,s}(E) \sim E^{-(\alpha_p - 0.1)}$$

$$\phi_{\gamma,diff}(E) \propto E^{-(\alpha_p - 0.1 + \delta)}$$



Diffuse Galactic gamma-ray emission:

$$\phi_{\gamma,tot} = \phi_{\gamma,s} + \phi_{\gamma,diff}$$

- The study of the diffuse emission is useful to constrain the CR transport properties in our Galaxy;
- Standard picture: CRs diffuse in our Galaxy and the diffusion coefficient is homogeneous throughout the Galaxy → CR properties are the same everywhere in the Galaxy;

$$D(E) \propto E^{\delta} \longrightarrow \phi_{\gamma,diff}(E) \propto E^{-(\alpha_p - 0.1 + \delta)}$$

Diffuse Galactic gamma-ray emission:

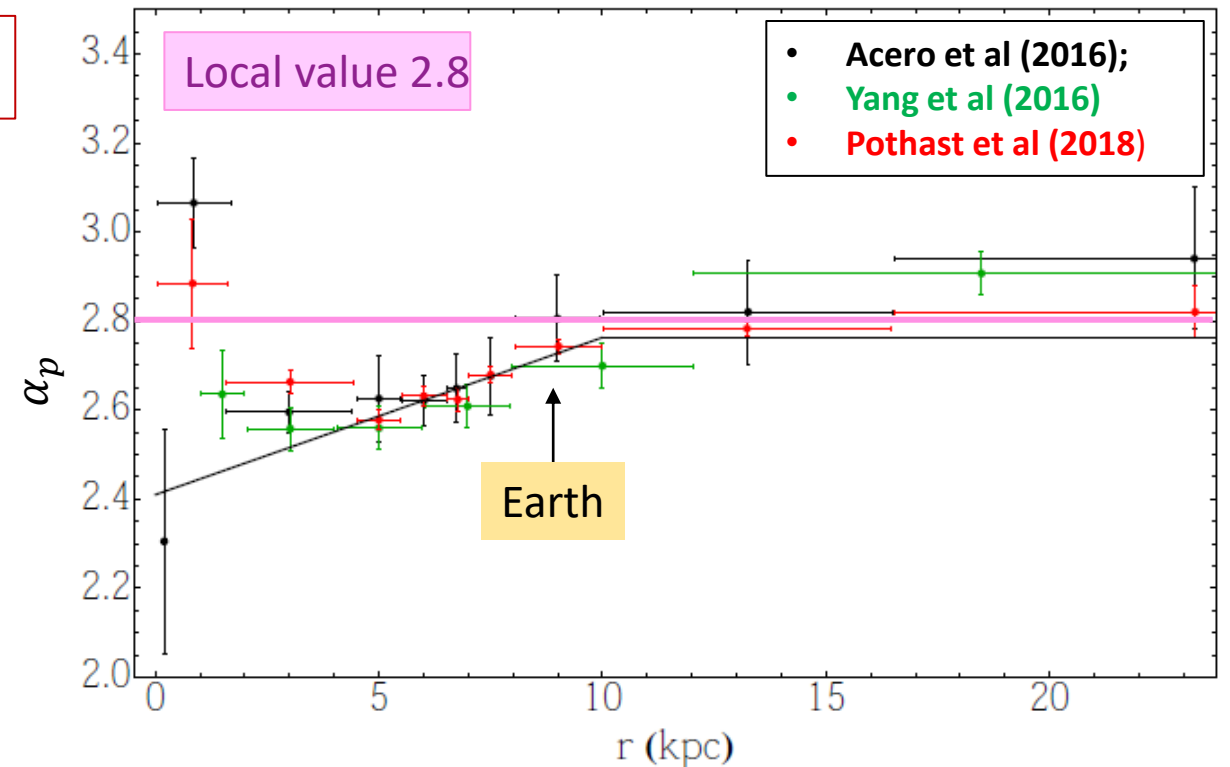
$$\phi_{\gamma,tot} = \phi_{\gamma,s} + \phi_{\gamma,diff}$$

- The study of the diffuse emission is useful to constrain the CR transport properties in our Galaxy;
- Standard picture: CRs diffuse in our Galaxy and the diffusion coefficient is homogeneous throughout the Galaxy → CR properties are the same everywhere in the Galaxy;

$$D(E) \propto E^\delta \longrightarrow \phi_{\gamma,diff}(E) \propto E^{-(\alpha_p - 0.1 + \delta)}$$

- Recent studies of the Fermi-LAT diffuse emission (GeV energy) have shown that the CR spectral index may depend on the Galactocentric radius: [Acero et al. \(2016\)](#), [Yang et al. \(2016\)](#), [Pothast et al. \(2018\)](#)

→ signature of non-standard CR propagation;



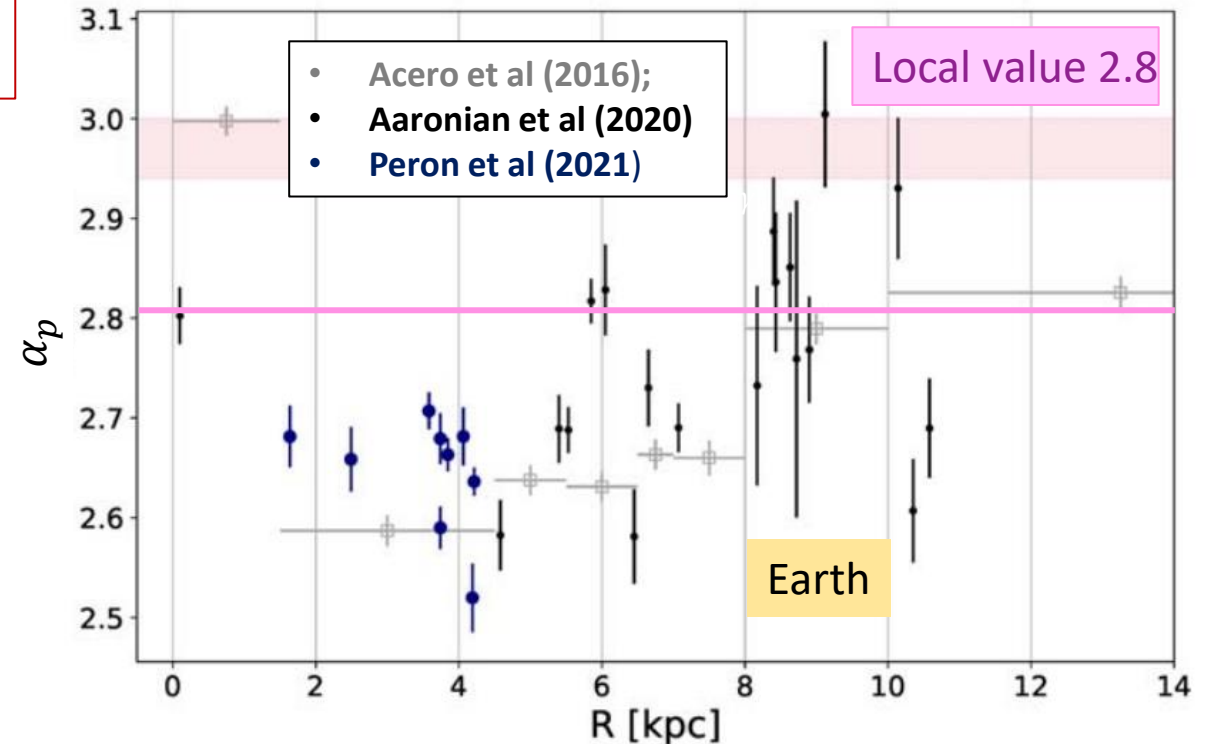
Diffuse Galactic gamma-ray emission:

$$\phi_{\gamma,tot} = \phi_{\gamma,s} + \phi_{\gamma,diff}$$

- The study of the diffuse emission is useful to constrain the CR transport properties in our Galaxy;
- Standard picture: CRs diffuse in our Galaxy and the diffusion coefficient is homogeneous throughout the Galaxy → CR properties are the same everywhere in the Galaxy;

$$D(E) \propto E^\delta \longrightarrow \phi_{\gamma,diff}(E) \propto E^{-(\alpha_p - 0.1 + \delta)}$$

- Molecular Clouds are the ideal environment to probe local CR properties: between 2 kpc - 6 kpc the CR spectral index appears scattered but still harder than the local one [Aharonian et al., PhRvD \(2020\)](#), [Peron et al., Astrophys. J \(2021\)](#);



Diffuse Galactic gamma-ray emission:

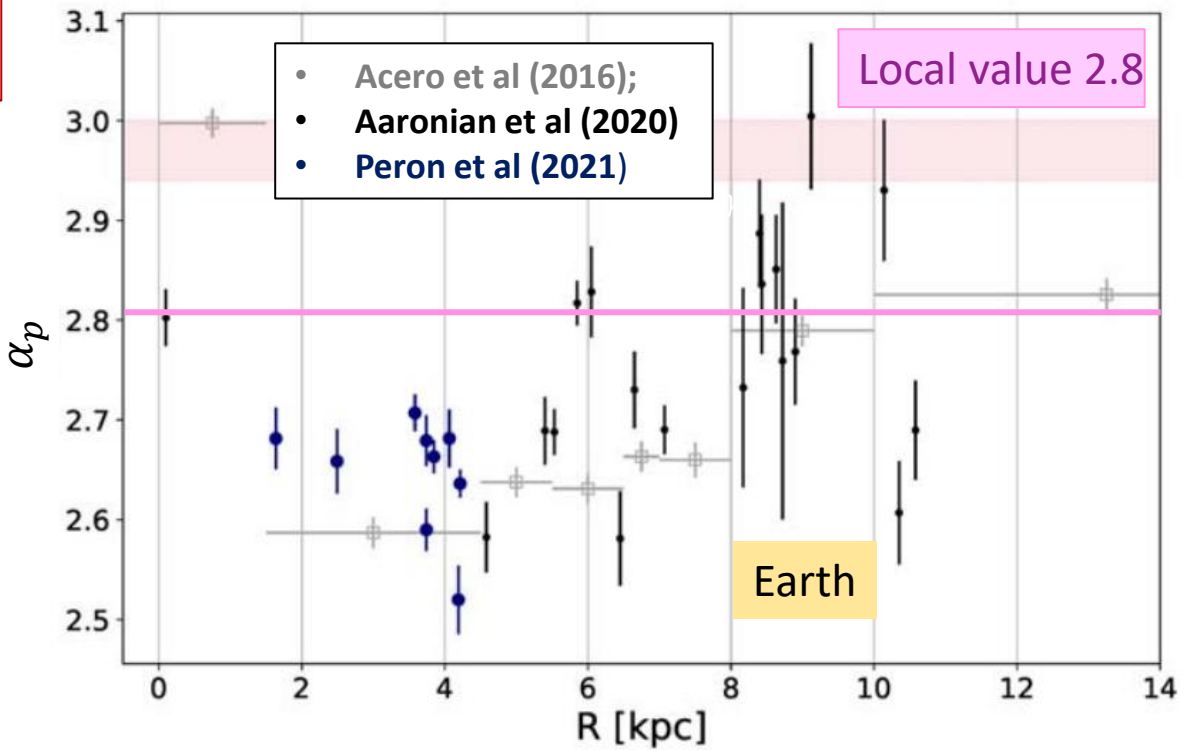
$$\phi_{\gamma,tot} = \phi_{\gamma,s} + \phi_{\gamma,diff}$$

- The study of the diffuse emission is useful to constrain the CR transport properties in our Galaxy;
- Standard picture: CRs diffuse in our Galaxy and the diffusion coefficient is homogeneous throughout the Galaxy → CR properties are the same everywhere in the Galaxy;

$$D(E) \propto E^\delta \rightarrow \phi_{\gamma,diff}(E) \propto E^{-(\alpha_p - 0.1 + \delta)}$$

- Molecular Clouds are the ideal environment to probe local CR properties: between 2 kpc - 6 kpc the CR spectral index appears scattered but still harder than the local one [Aharonian et al., PhRvD \(2020\)](#), [Peron et al., Astrophys. J \(2021\)](#);

New measurement at higher energy: H.E.S.S., Tibet AS γ , HAWC and LHAASO;



Unresolved sources:

$$\phi_{\gamma,tot} = \phi_{\gamma,s} + \phi_{\gamma,diff}$$

Measured $\phi_{\gamma,tot}$

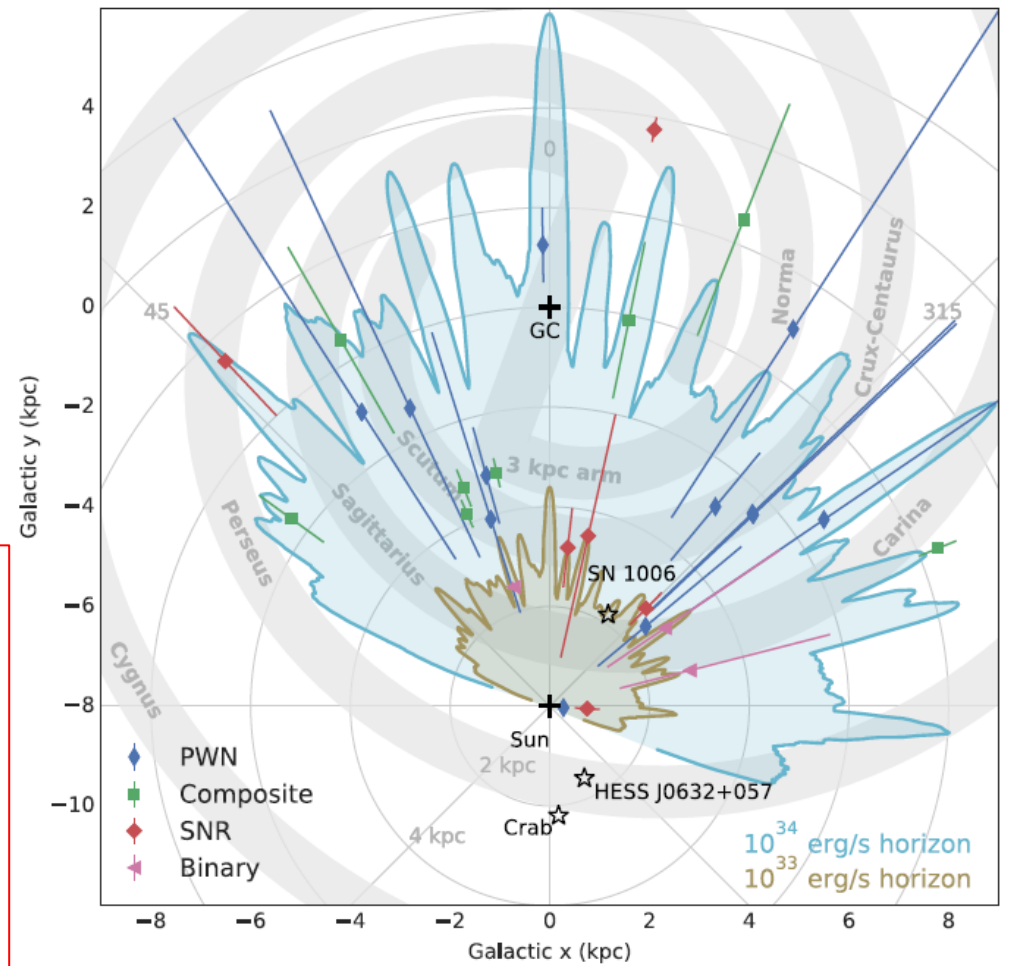
$$\phi_{\gamma,s}^r + \phi_{\gamma,s}^{unr}$$

Detectors can resolve only a fraction of Galactic sources due to their limited sensitivity threshold \rightarrow unresolved sources;

The Galactic diffuse gamma-ray emission provided by experiments is obtained by masking the contribution of known sources \rightarrow unresolved sources contribute to the measured diffuse emission

If not negligible \rightarrow it changes the interpretation of data

H.E.S.S. Collaboration: The H.E.S.S. Galactic plane survey



Outline:

- Population study of the H.E.S.S. Galactic Plane Survey (HGPS) under the hypothesis that the signal is dominated by pulsar-powered sources;

Cataldo et al. Astrophys.J. (2020)

Vecchiotti et al, ICRC 2021, Journal of Physics: Conference Series.

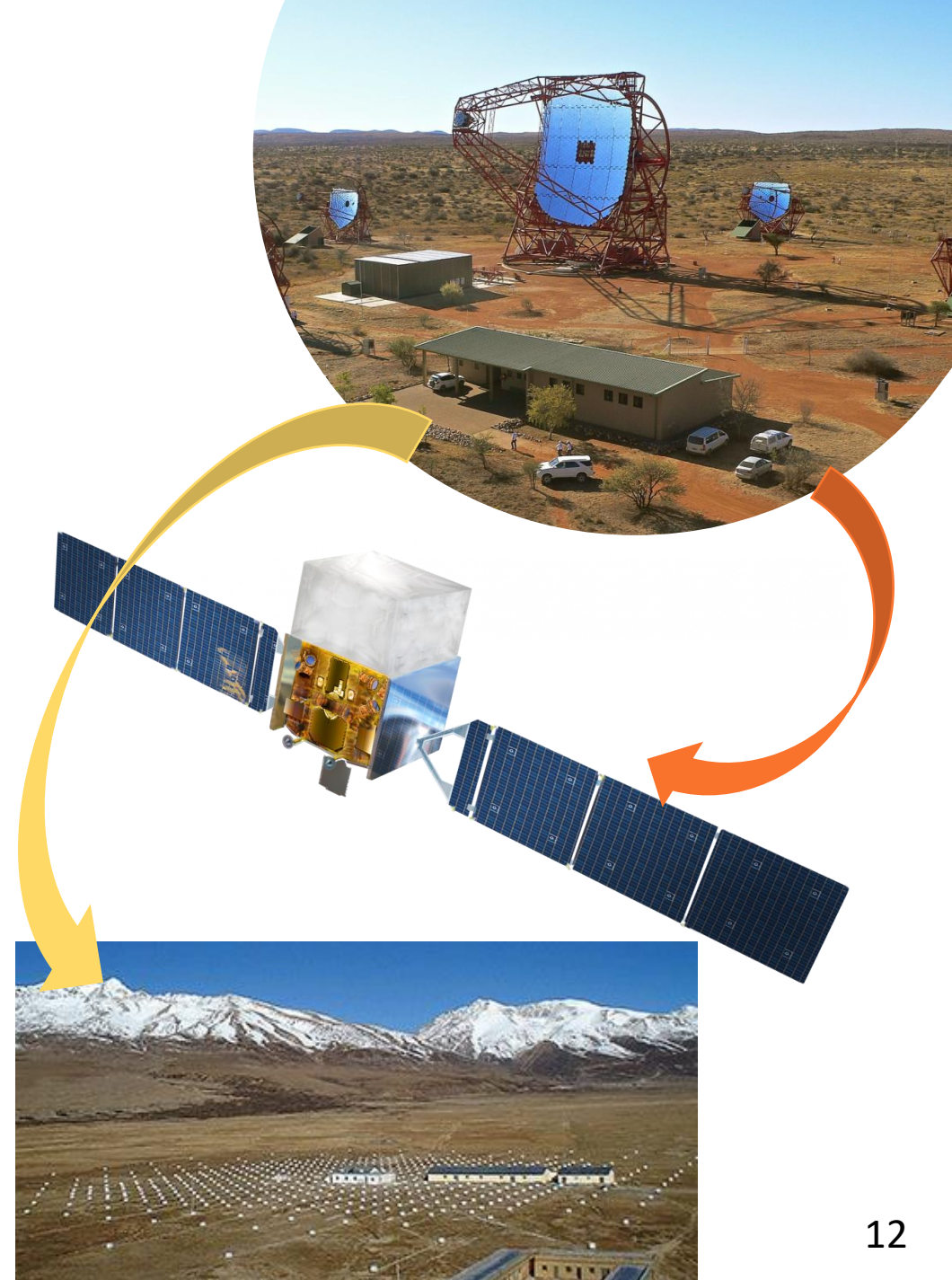
- Prediction in the **GeV energy** range (Fermi-LAT)

Vecchiotti et al, Communication Physics. (2022)

Pagliaroli et al, ICRC 2021, Journal of Physics: Conference Series.

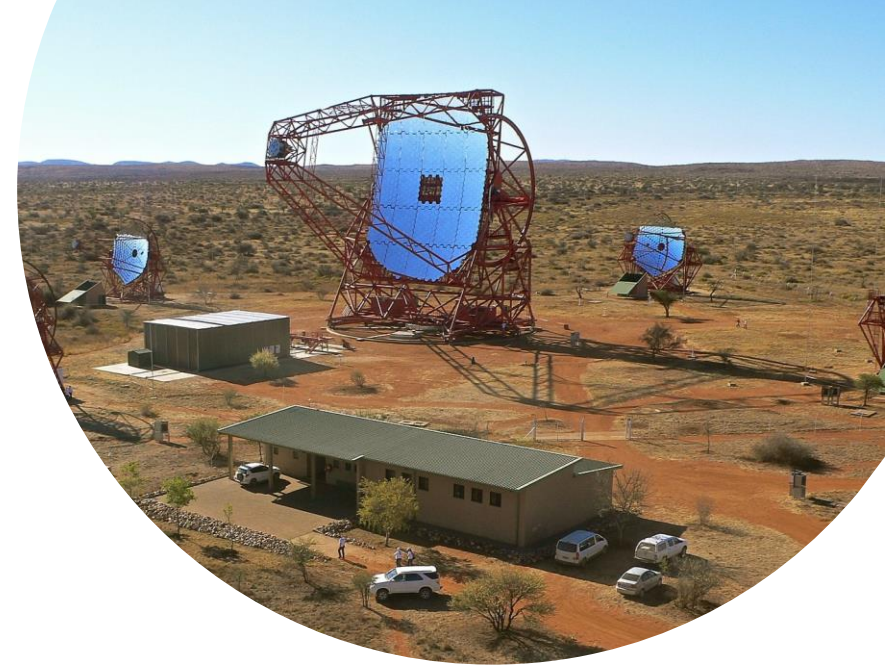
- Prediction in the **sub-PeV energy** range (Tibet AS γ)

Vecchiotti et al, Astrophys. J. (2022)



Population studies of TeV sources

Cataldo et al. *Astrophys.J.* 904 (2020)

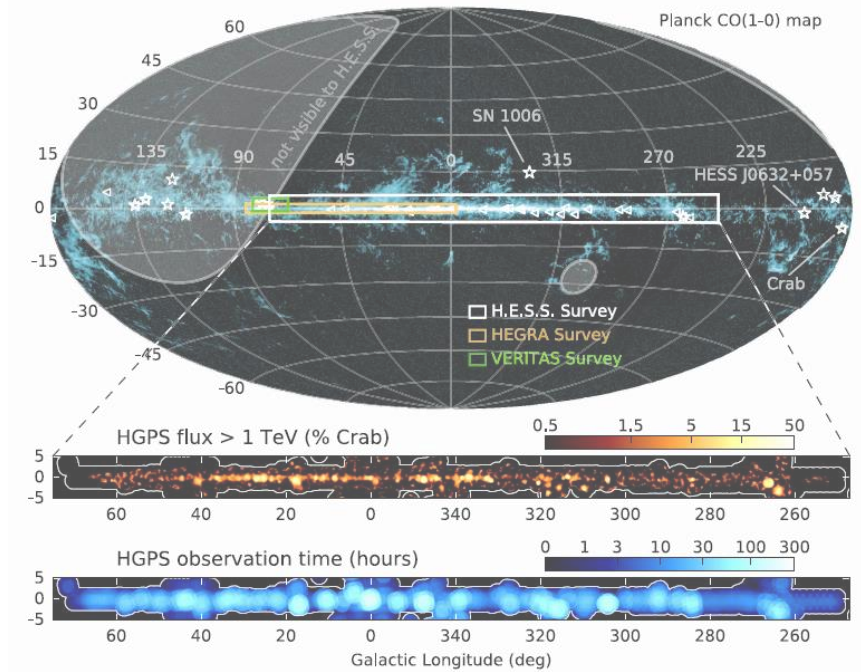


Study of the Pulsar wind nebulae population in the TeV range:

Cataldo et al. *Astrophys.J.* 904 (2020)

- The HGPS catalogue ($\phi > 0.1\phi_{Crab}$);

Abdalla et al, *A&A*, 612, A1 (2018)



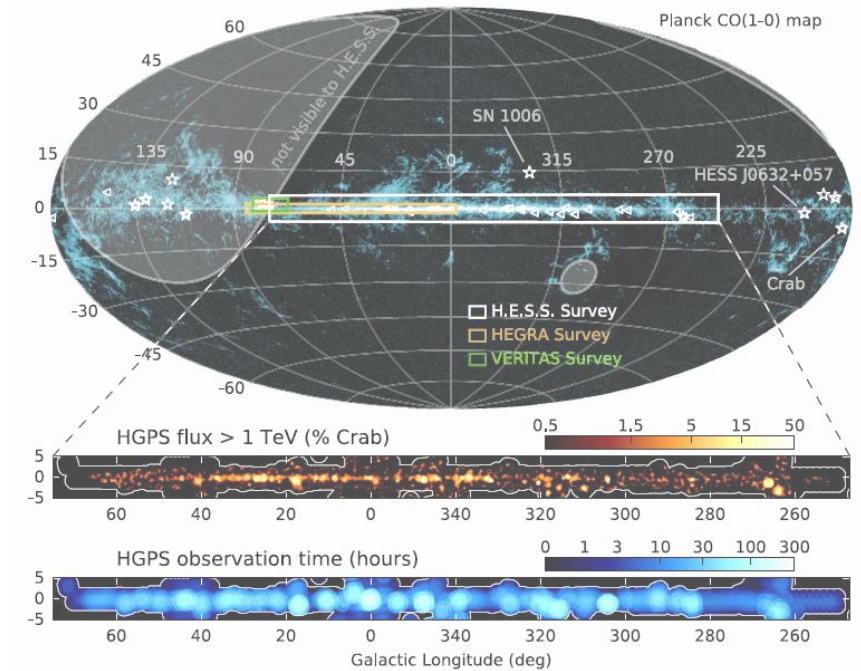
Study of the Pulsar wind nebulae population in the TeV range:

Cataldo et al. *Astrophys.J.* 904 (2020)

- The HGPS catalogue ($\phi > 0.1\phi_{Crab}$);
- Model for TeV source population:
we assume the **spatial distribution** and the **luminosity distribution** of the sources;

$$\frac{dN}{d^3r dL} = \rho(r)Y(L)$$

Abdalla et al, *A&A*, 612, A1 (2018)

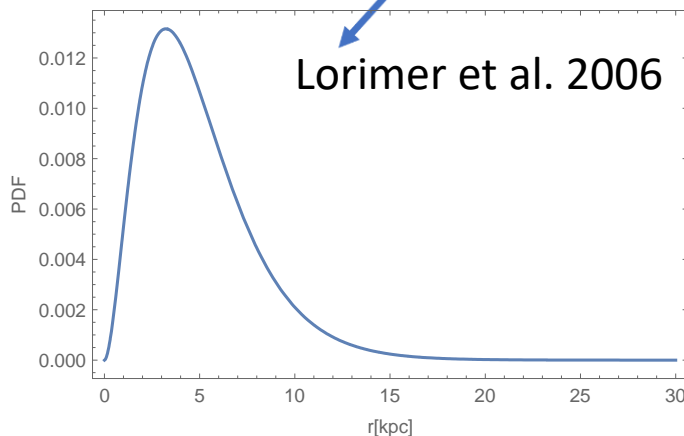


Study of the Pulsar wind nebulae population in the TeV range:

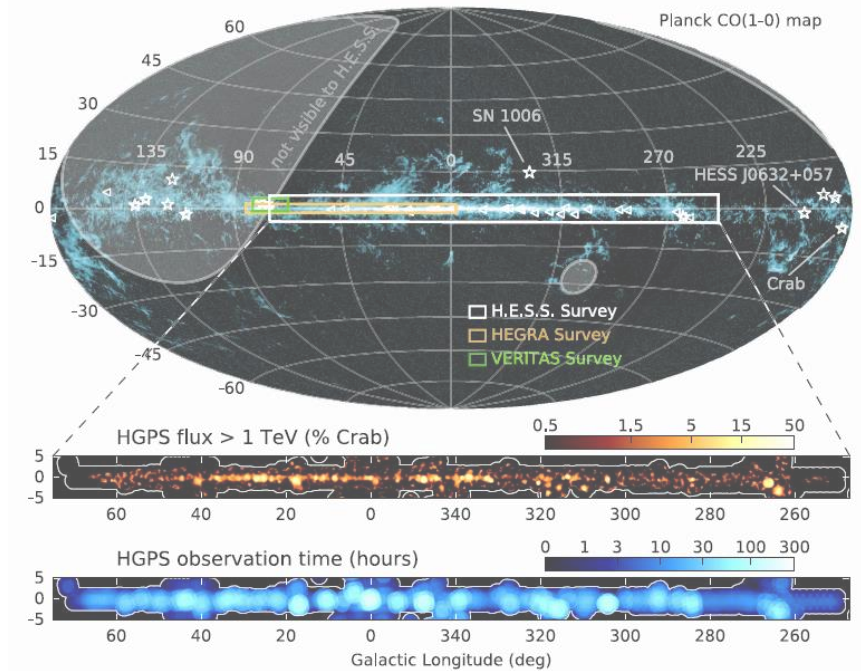
Cataldo et al. *Astrophys.J.* 904 (2020)

- The HGPS catalogue ($\phi > 0.1\phi_{Crab}$);
- Model for TeV source population:
we assume the **spatial distribution** and the **luminosity distribution** of the sources;

$$\frac{dN}{d^3r dL} = \rho(r) Y(L)$$



Abdalla et al, *A&A*, 612, A1 (2018)

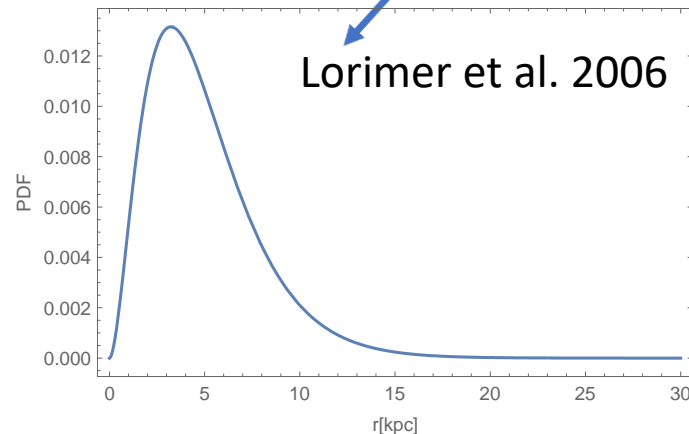


Study of the Pulsar wind nebulae population in the TeV range:

Cataldo et al. *Astrophys.J.* 904 (2020)

- The HGPS catalogue ($\phi > 0.1\phi_{Crab}$);
- Model for TeV source population:
we assume the **spatial distribution** and the **luminosity distribution** of the sources;

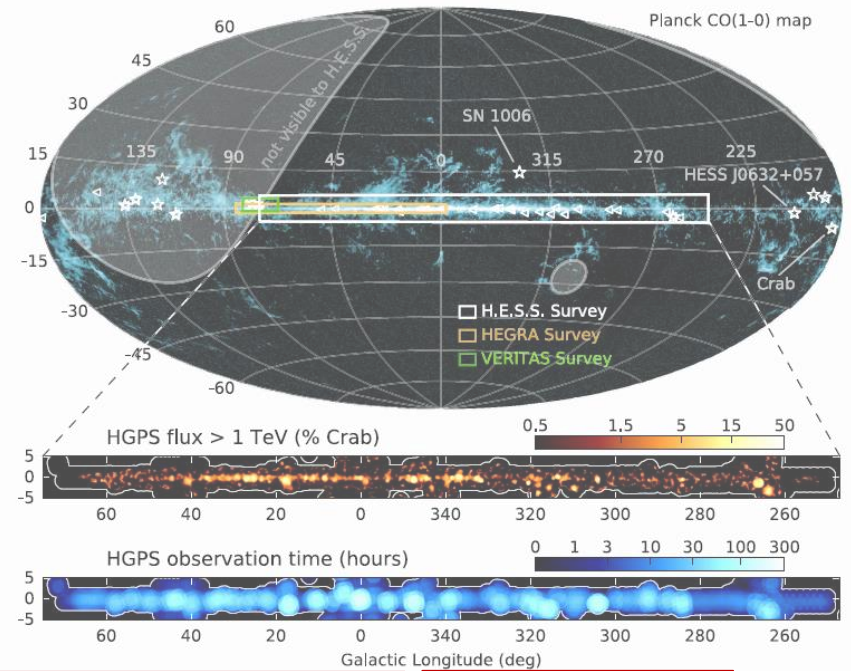
$$\frac{dN}{d^3r dL} = \rho(r) Y(L)$$



$$Y(L) = \frac{R \tau (\alpha - 1)}{L_{\max}} \left(\frac{L}{L_{\max}} \right)^{-\alpha}$$

$\alpha = 1.5$
 $\alpha = 1.8$

$\alpha = 1/\gamma + 1$ For pulsar-powered sources:
 $R = 0.019 \text{ yr}^{-1}$ $L(t) = L_{\max} \left(1 + \frac{t}{\tau} \right)^{-\gamma}$

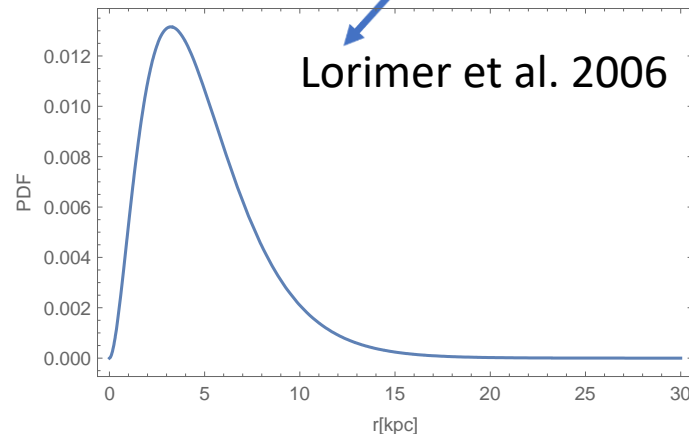


Study of the Pulsar wind nebulae population in the TeV range:

Cataldo et al. *Astrophys.J.* 904 (2020)

- The HGPS catalogue ($\phi > 0.1\phi_{Crab}$);
- Model for TeV source population:
we assume the **spatial distribution** and the **luminosity distribution** of the sources;

$$\frac{dN}{d^3r dL} = \rho(r) Y(L)$$



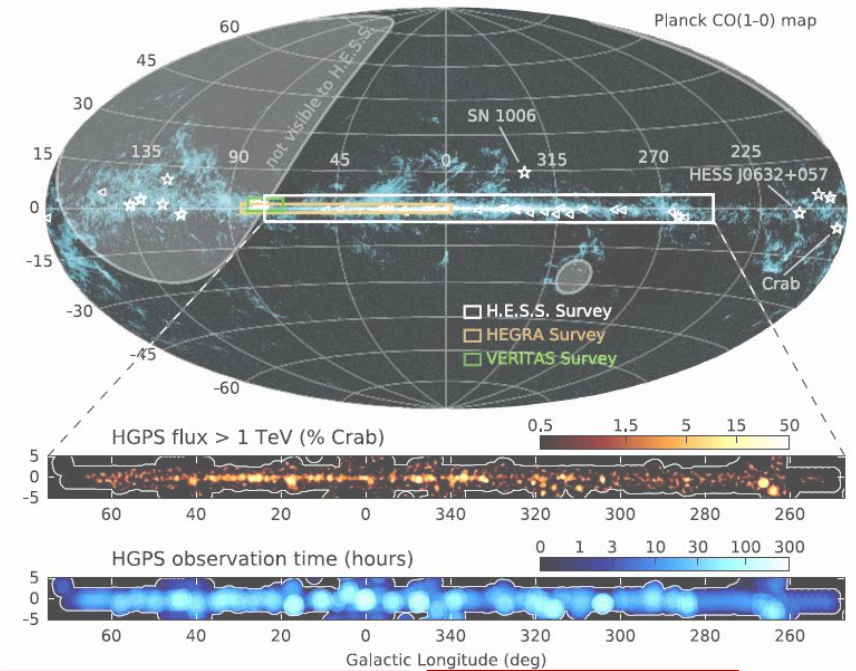
$$Y(L) = \frac{R \tau (\alpha - 1)}{L_{\max}} \left(\frac{L}{L_{\max}} \right)^{-\alpha}$$

$\alpha = 1.5$
 $\alpha = 1.8$

$\alpha = 1/\gamma + 1$ For pulsar-powered sources:

$R = 0.019 \text{ yr}^{-1}$ $L(t) = L_{\max} \left(1 + \frac{t}{\tau} \right)^{-\gamma}$

We assume a **power-law** energy spectrum with index $\beta_{TeV} = 2.3$ that is the average index for all the sources in the HGPS catalogue.



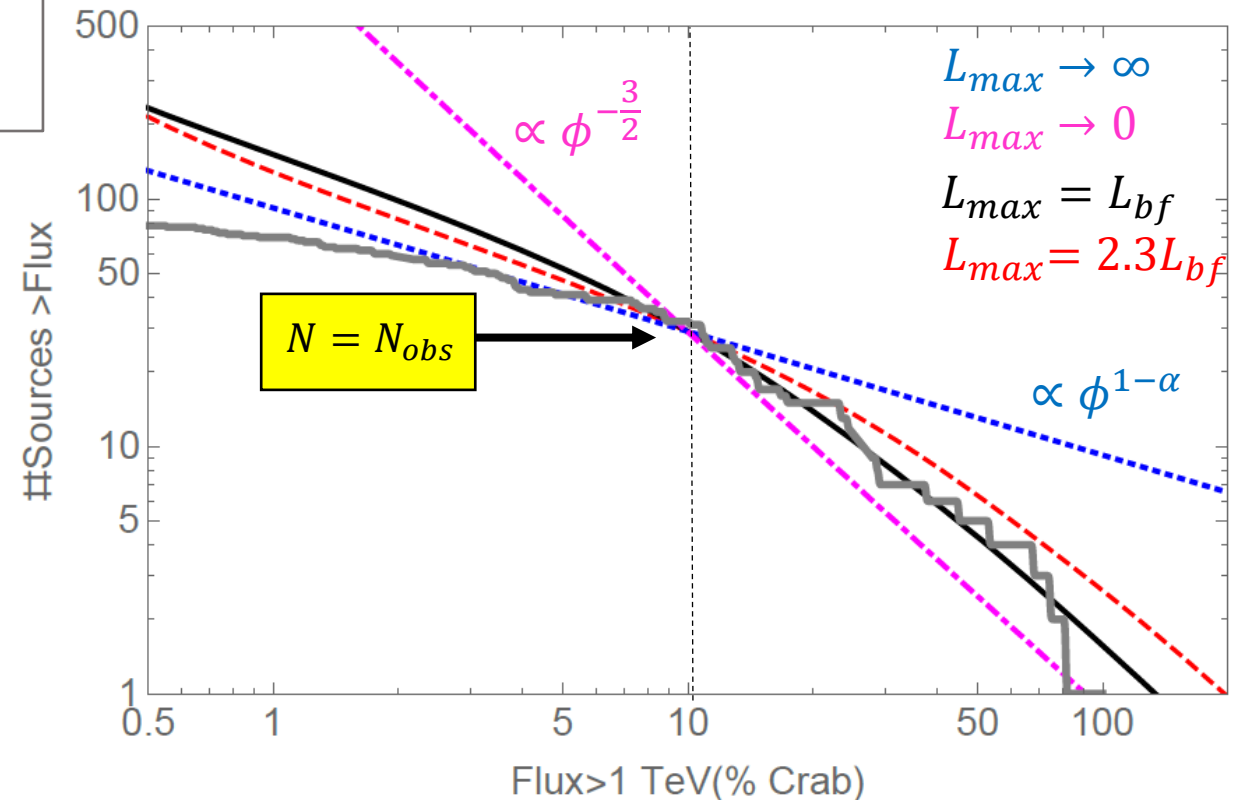
Study of the Pulsar wind nebulae population in the TeV range:

Cataldo et al. *Astrophys.J.* 904 (2020)

We fit the H.E.S.S. observational results with an unbinned likelihood

$$\alpha = 1.5$$

$$L_{max} = 4.0^{+3.0}_{-2.1} \times 10^{35} \text{ erg s}^{-1}$$
$$\tau = 1.8^{+1.5}_{-0.6} \text{ kyr}$$



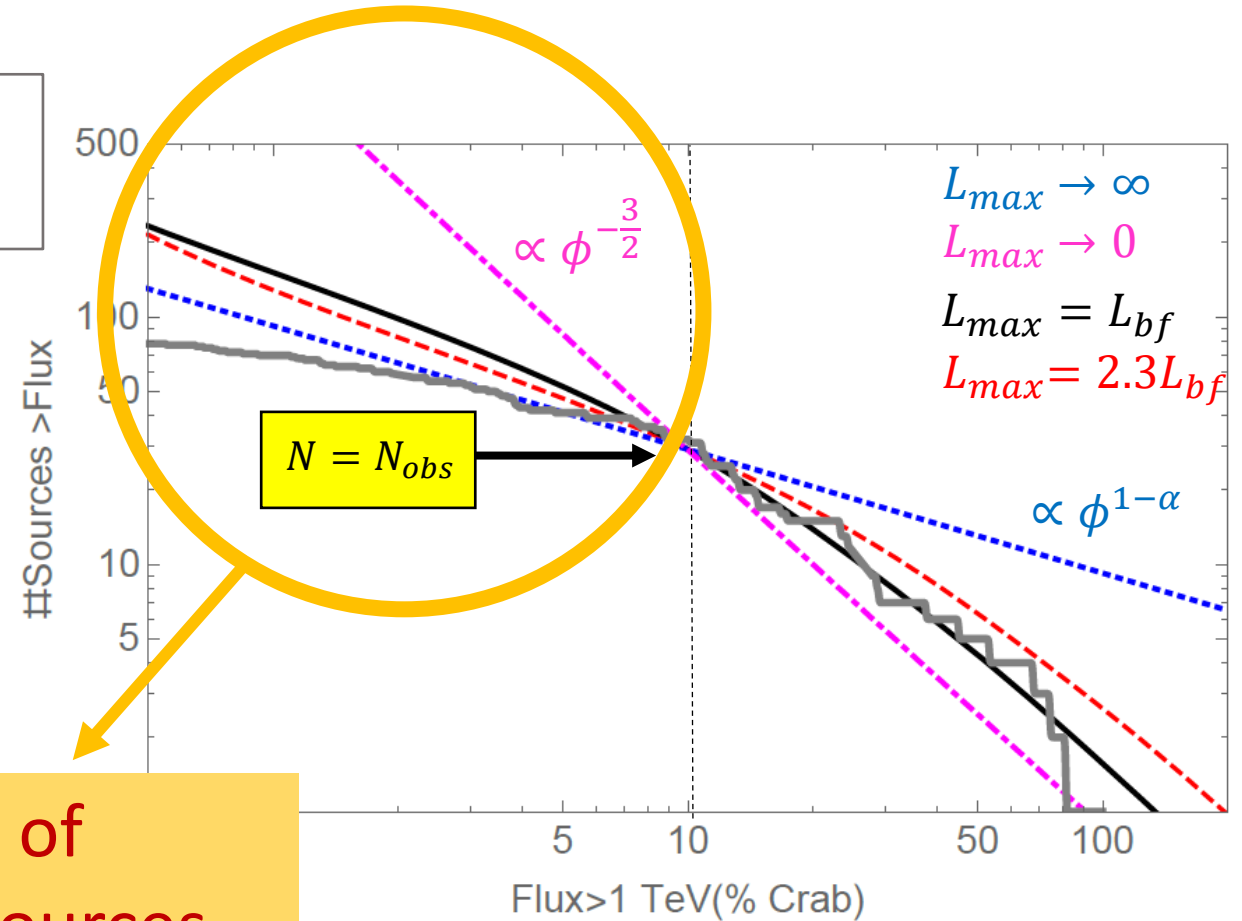
Study of the Pulsar wind nebulae population in the TeV range:

Cataldo et al. *Astrophys.J.* 904 (2020)

We fit the H.E.S.S. observational results with an unbinned likelihood

$$\alpha = 1.5$$

$$L_{max} = 4.0^{+3.0}_{-2.1} \times 10^{35} \text{ erg s}^{-1}$$
$$\tau = 1.8^{+1.5}_{-0.6} \text{ kyr}$$



Contribution of unresolved sources

Results:

- The total **TeV luminosity (1-100 TeV)** of the Galaxy:

$$L_{MW} = \frac{R\tau(\alpha-1) L_{max}}{(2-\alpha)} \left[1 - \left(\frac{L_{min}}{L_{max}} \right)^{\alpha-2} \right] = 1.7_{-0.4}^{+0.5} \times 10^{37} \text{ erg s}^{-1}$$

- The total **flux at Earth produced by all sources (1-100 TeV)** (resolved and unresolved) in the H.E.S.S. OW:

$$\phi_{tot} = \frac{L_{MW}}{4\pi \langle E \rangle} \int_{OW} d^3r \rho(r) r^{-2} = 3.8_{-1.0}^{+1.0} \times 10^{-10} \text{ cm}^{-2} \text{ s}^{-1}$$

3.25 TeV

- By subtraction we can obtain the contribution of **unresolved sources**:

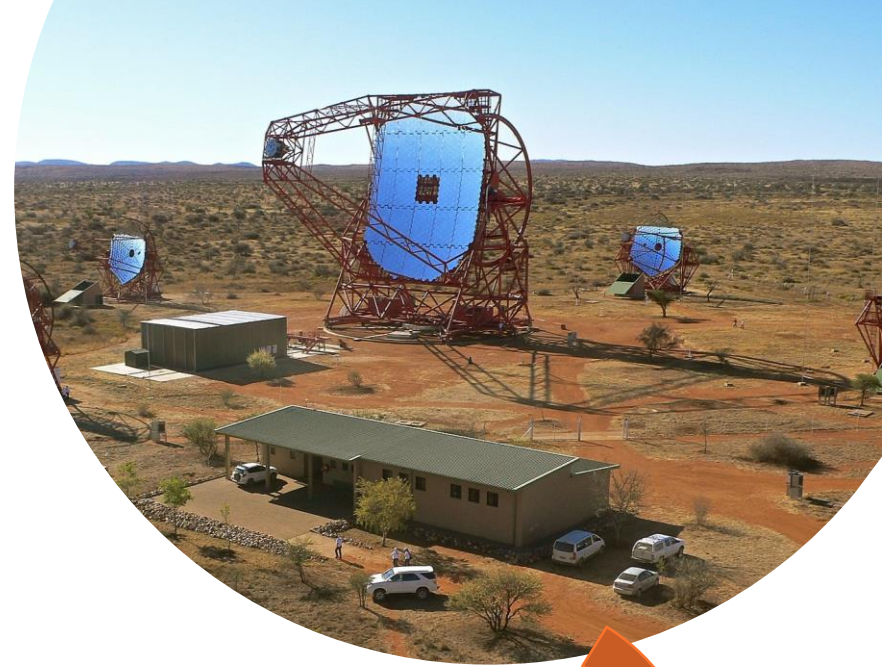
$$\phi_S^{unr} = \phi_{tot}(< 0.1 \phi_{Crab}) - \phi_S^r(< 0.1 \phi_{Crab}) \sim 40\% \phi_S^r$$

Take home message:

- The contribution of unresolved sources is not negligible being $\sim 40\%$ of the resolved signal measured by H.E.S.S.;

GeV energy range

Vecchiotti et al, Communication Physics. (2022)



Implications of TeV PWNe at GeV energy range:

- TeV PWNe are expected to emit also at lower energies (subdominant class of sources since the Galactic GeV source population is dominated by pulsars);
- Some of them produce a signal that remains unresolved for Fermi-LAT
- Impact of unresolved TeV PWNe in the interpretation of the measured Fermi-LAT large-scale diffuse emission

$$\phi_{\gamma,S}^{NR} + \phi_{\gamma,diff} \longrightarrow \text{Measured}$$

Unresolved TeV PWNe and the hadronic diffuse emission add up and shape the radial and spectral behaviours of the total diffuse gamma ray emission observed by Fermi-LAT

Extrapolate to GeV range:

We define the phenomenological parameter: $R_{\Phi} = \frac{\Phi_{\text{GeV}}}{\Phi_{\text{TeV}}}$

We can calculate the total source flux and the unresolved sources in the energy range 1-100 GeV using our knowledge of the 1-100 TeV energy range:

$$\phi_{\text{GeV}}^{\text{tot}} = R_{\phi} \phi_{\text{TeV}}^{\text{tot}}$$
$$\frac{dN}{d\phi_{\text{GeV}}} = \frac{1}{R_{\phi}} \frac{dN}{d\phi_{\text{TeV}}} \left(\frac{\phi_{\text{GeV}}}{R_{\phi}} \right) \rightarrow \phi_{\text{GeV}}^{\text{NR}} = \int_0^{\phi_{\text{GeV}}^{\text{th}}} d\phi_{\text{GeV}} \phi_{\text{GeV}} \frac{dN}{d\phi_{\text{GeV}}} \propto R_{\phi}^{\alpha-1}$$

Extrapolate to GeV range:

We define the phenomenological parameter: $R_\Phi = \frac{\Phi_{\text{GeV}}}{\Phi_{\text{TeV}}}$

We can calculate the total source flux and the unresolved sources in the energy range 1-100 GeV using our knowledge of the 1-100 TeV energy range:

$$\phi_{\text{GeV}}^{\text{tot}} = R_\phi \phi_{\text{TeV}}^{\text{tot}}$$
$$\frac{dN}{d\phi_{\text{GeV}}} = \frac{1}{R_\phi} \frac{dN}{d\phi_{\text{TeV}}} \left(\frac{\phi_{\text{GeV}}}{R_\phi} \right) \rightarrow \phi_{\text{GeV}}^{\text{NR}} = \int_0^{\phi_{\text{GeV}}^{\text{th}}} d\phi_{\text{GeV}} \phi_{\text{GeV}} \frac{dN}{d\phi_{\text{GeV}}} \propto R_\phi^{\alpha-1}$$

We need a spectral assumption (motivated by observation):

$$\varphi_{\text{PWN}}(E) = \varphi_0 \begin{cases} \left(\frac{E}{E_b} \right)^{-\beta_{\text{GeV}}} & E \leq E_b \\ \left(\frac{E}{E_b} \right)^{-\beta_{\text{TeV}}} & E > E_b \end{cases}$$

$$R_\phi, E_b, \beta_{\text{TeV}} \rightarrow \beta_{\text{GeV}}$$

Parameter space:

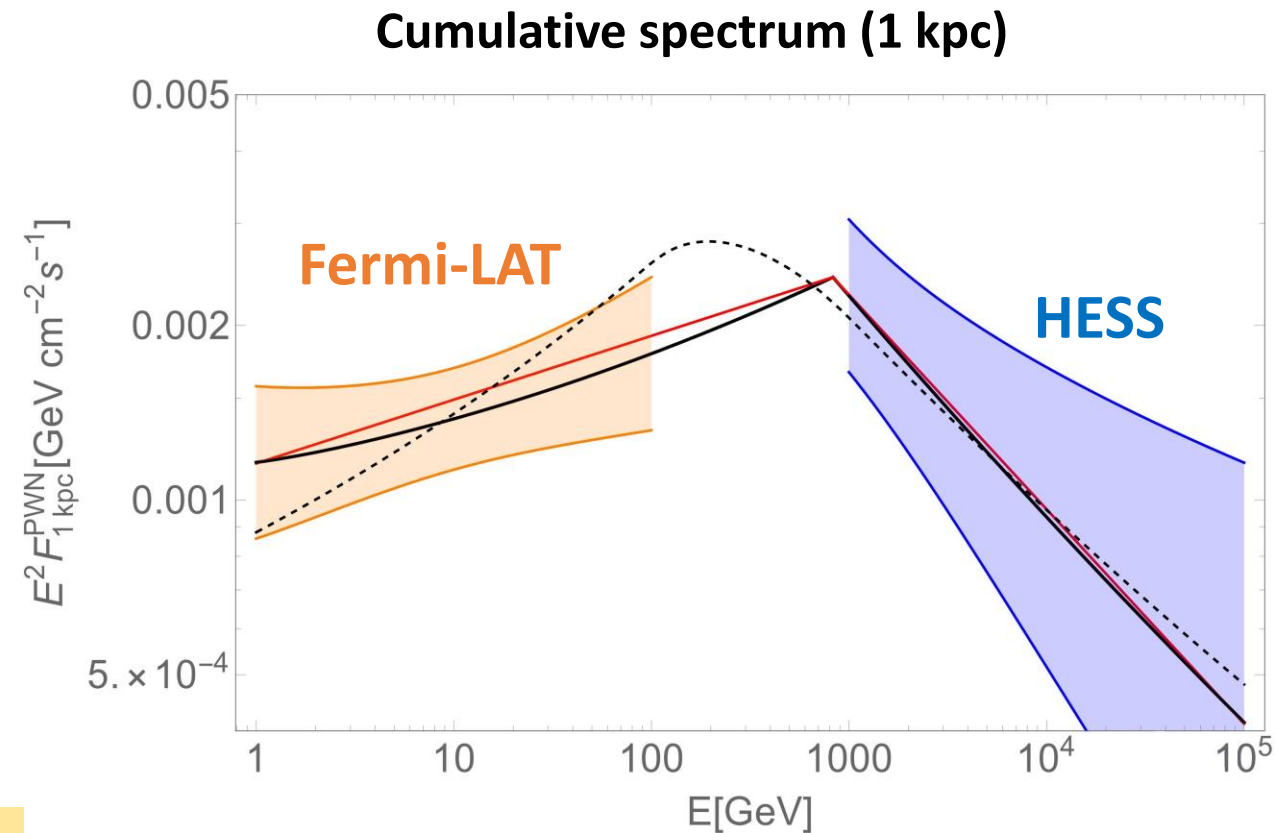
Properties of 12 objects firmly identified as PWNe by both HGPS (*Abdalla et al, A&A, 612, A1 (2018)*) and 4FGL-DR2 (*Abdollahi et Al, Astrophys. J. Suppl. 247 (2020)*)

- $R_\phi = [250 - 1500]$;
- $E_0 = [0.1 - 1]$ TeV;
- $\beta_{TeV} = [1.9 - 2.5]$;
- $\beta_{GeV}(R_\phi, E_0, \beta_{TeV}) = [1.06 - 2.19]$

Cumulative spectrum of sources with known distance;

Average spectrum (red line):

$$\beta_{TeV} = 2.4, E_b \sim 0.8 \text{ TeV}, R_\phi \sim 770, \rightarrow \beta_{GeV} \sim 1.9$$



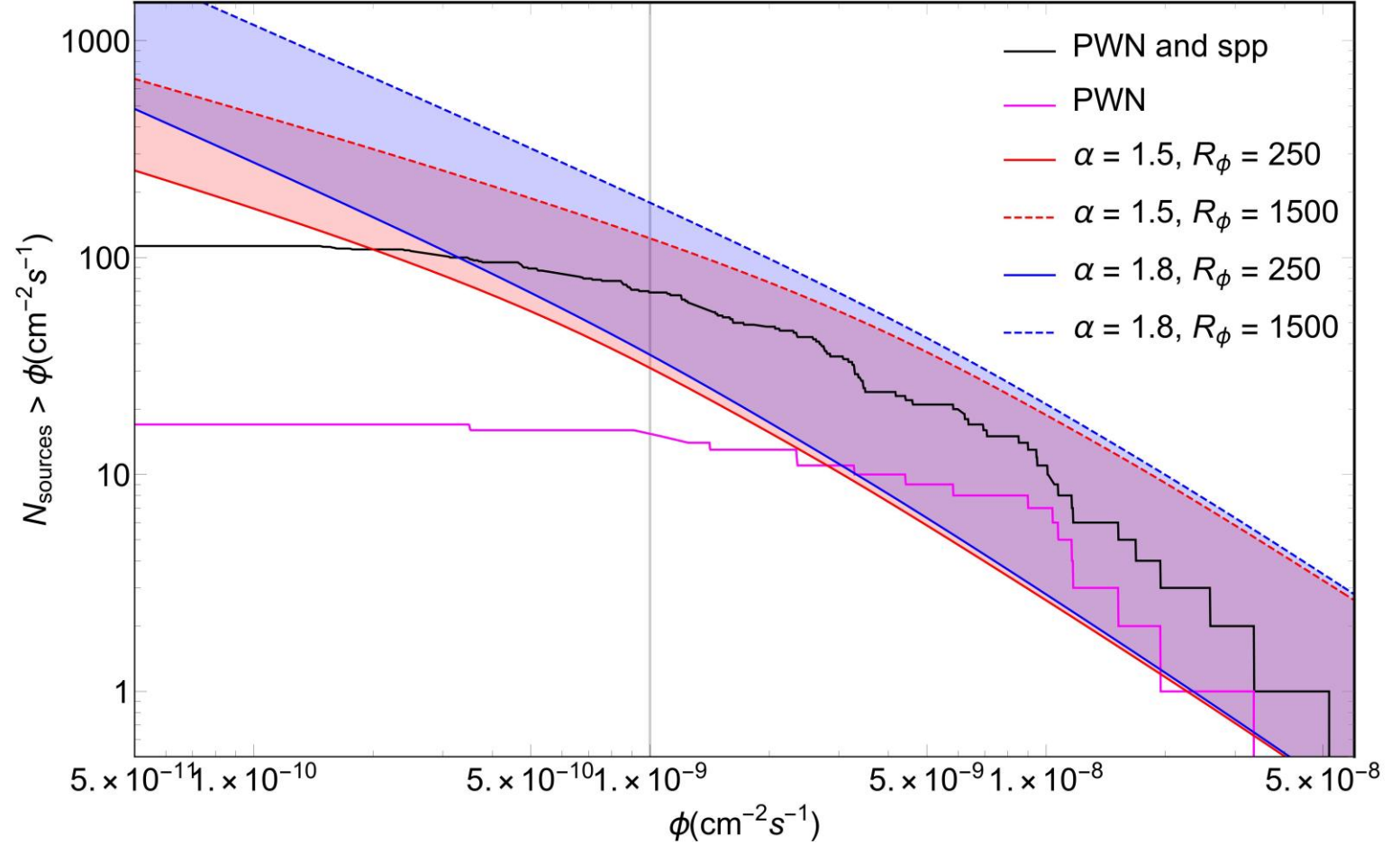
Unresolved PWNe by Fermi-LAT:

$$\alpha = 1.8$$

$$\frac{\phi_{NR}}{\phi_{PWN}} = (32\% - 46\%)$$

$$\alpha = 1.5$$

$$\frac{\phi_{NR}}{\phi_{PWN}} = (10\% - 24\%)$$



$$\Phi_{\text{GeV}}^{\text{th}} = 10^{-9} \text{ cm}^{-2} \text{ s}^{-1} \quad \text{Acero et.al. 2015}$$

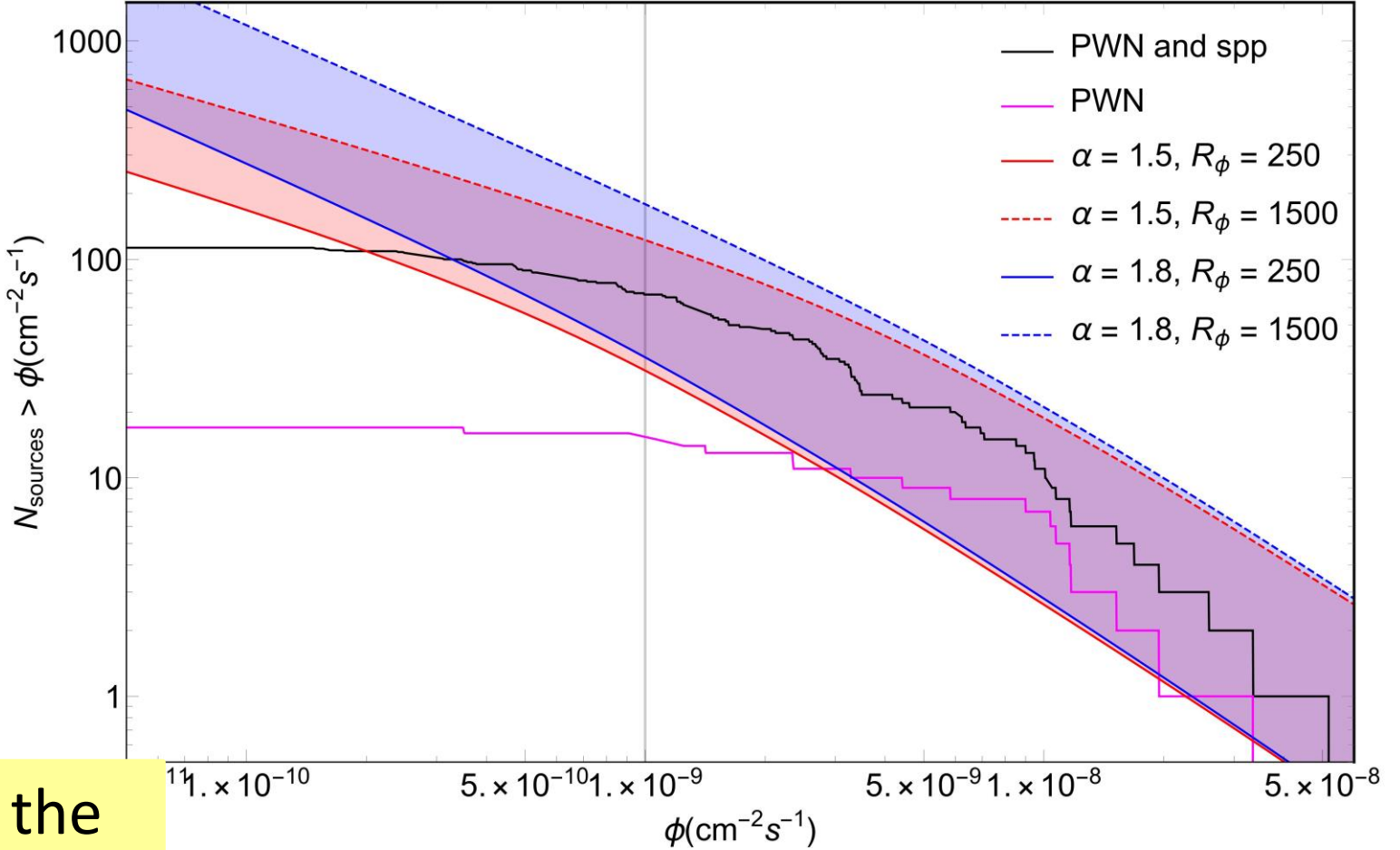
Unresolved PWNe by Fermi-LAT:

$$\alpha = 1.8$$

$$\frac{\phi_{NR}}{\phi_{PWN}} = (32\% - 46\%)$$

$$\alpha = 1.5$$

$$\frac{\phi_{NR}}{\phi_{PWN}} = (10\% - 24\%)$$



A non-negligible fraction of the TeV PWNe population cannot be resolved by Fermi-LAT

$$\Phi_{\text{GeV}}^{\text{th}} = 10^{-9} \text{ cm}^{-2} \text{ s}^{-1} \quad \text{Acero et.al. 2015}$$

Reinterpreting the diffuse emission observed by Fermi-LAT:

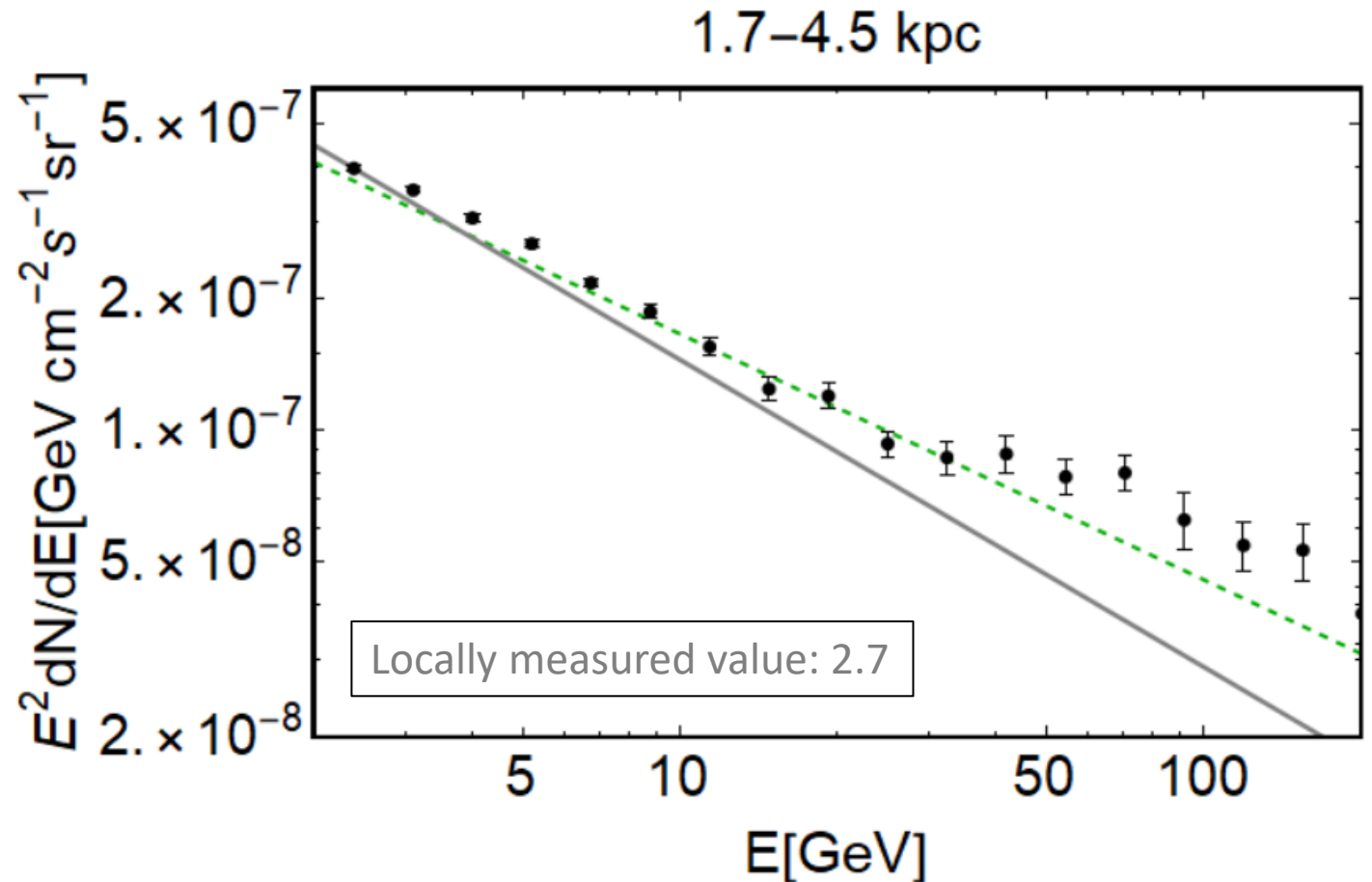
The unresolved PWNe account up to the 36 % of the total diffuse emission in the ring 1.7-4.5 kpc.

Reinterpreting the diffuse emission observed by Fermi-LAT:

The unresolved PWNe account up to the 36 % of the total diffuse emission in the ring 1.7-4.5 kpc.

Diffuse emission (Power-Law):

$$\Gamma_1 = 2.56$$



Reinterpreting the diffuse emission observed by Fermi-LAT:

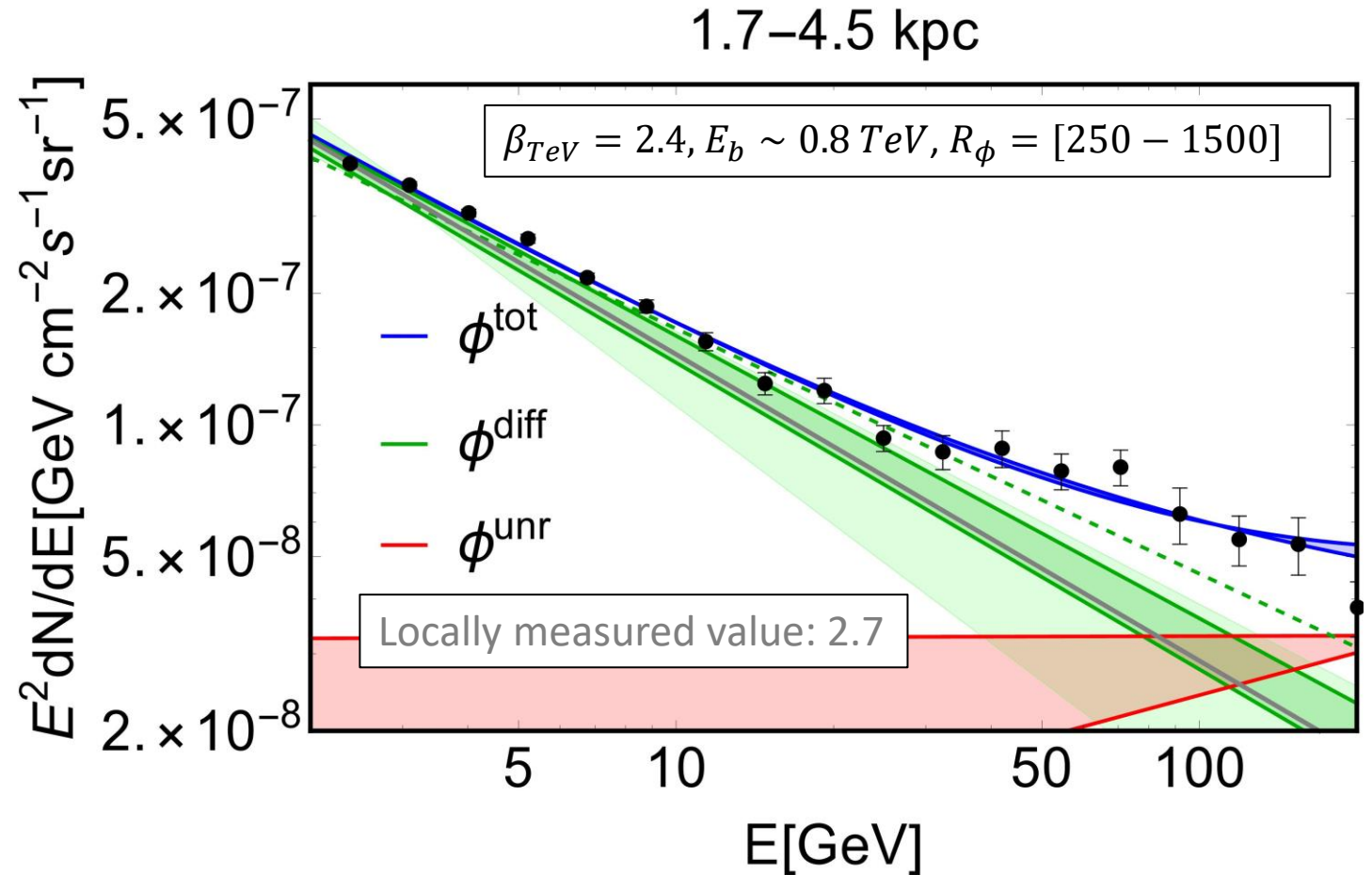
The unresolved PWNe account up to the 36 % of the total diffuse emission in the ring 1.7-4.5 kpc.

Diffuse emission (Power-Law):

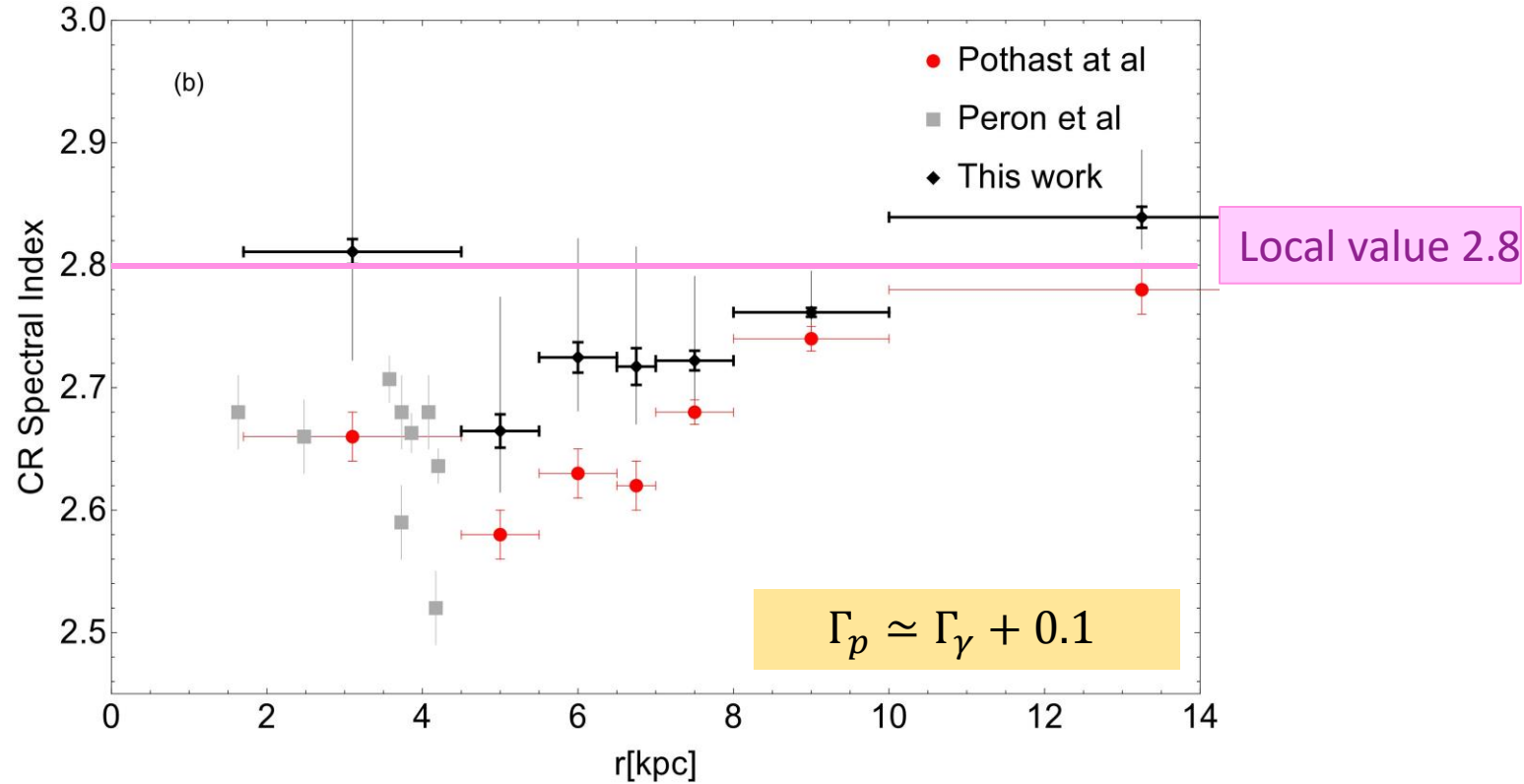
$$\Gamma_1 = 2.56$$

Diffuse emission (Power-Law)
+ Unresolved PWNe

$$\Gamma_{BF} = 2.64 - 2.71$$



Spectral index and gamma-ray emissivity ($\alpha = 1.8$):



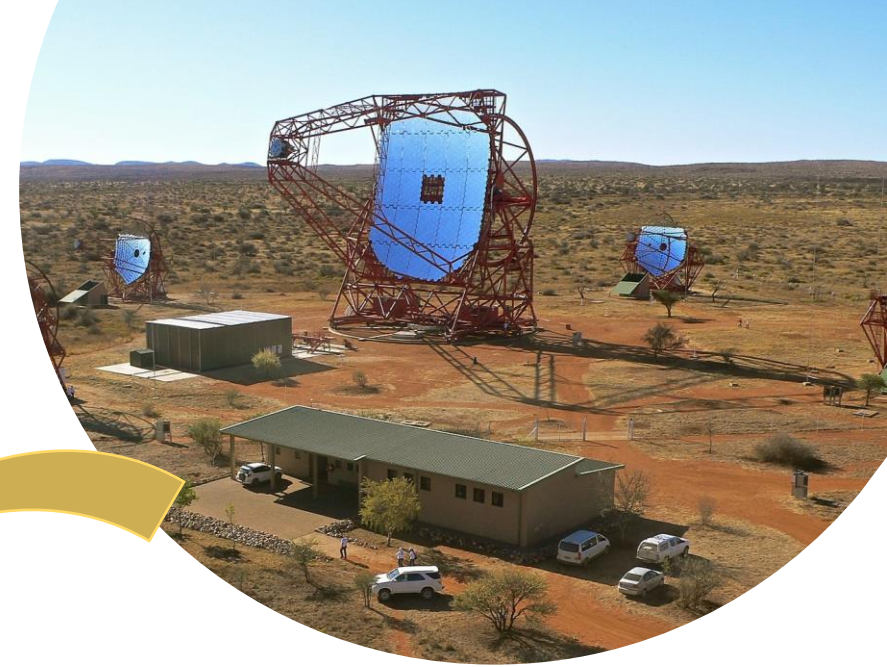
- PWNe contribution accounts for a part of the spectral index variation observed by Fermi-LAT in particular in the inner Galaxy;

Take home message:

- A non-negligible fraction of the TeV PWNe population cannot be resolved by Fermi-LAT
- TeV unresolved PWNe contribution could account for a part of the spectral index variation observed by Fermi-LAT in particular in the inner Galaxy;

Sub PeV energy range

Vecchiotti et al, Astrophys. J. (2022)



Tibet $AS\gamma$:

Amenomori, M., et al. 2021, Phys. Rev. Lett., 126, 141101,326

$\phi_{\gamma, \text{diff}}^{\text{Tibet}}$

First measurement of the Galactic diffuse γ -ray emission in the sub-PeV energy range.

They exclude the contribution from the known TeV sources (within 0.5 degrees) listed in the TeV source catalog.



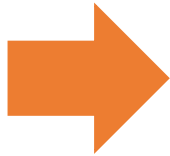
Tibet $AS\gamma$:

Amenomori, M., et al. 2021, Phys. Rev. Lett., 126, 141101,326

$\phi_{\gamma,diff}^{Tibet}$



First measurement of the Galactic diffuse γ -ray emission in the sub-PeV energy range.



They exclude the contribution from the known TeV sources (within 0.5 degrees) listed in the TeV source catalog.



The Tibet measurements are contaminated by the presence of Unresolved Sources

$\phi_{\gamma,diff}^{Tibet}$

=

$\phi_{\gamma,S}^{UnRes}$

+

$\phi_{\gamma,diff}$

Population study
(H.E.S.S.) \rightarrow we obtain general
information on the sources

Models:
Assumptions on the CR spatial
and energy distributions.

Diffuse Galactic γ and ν emission:

Cataldo et al. Astrophys.J. (2020)

$$\varphi_i^{diff}(E_i, \hat{n}_i) = A_i \int_{E_i}^{\infty} dE \frac{d\sigma(E, E_i)}{dE_i} \int_0^{\infty} dl \varphi_{CR}(E, \bar{r}_{Sun} + l\hat{n}_i) n_H(\bar{r}_{Sun} + l\hat{n}_i)$$

Where: $A_\gamma=1$ and $A_\nu=1/3$ (due to neutrino oscillation)

Differential inelastic cross section of pp interaction from the SYBILL code
[*Kelner, Aharonian, Bugayov (2006)*]

Cosmic-ray energy and spatial distribution

Interstellar gas distribution in the Galaxy [*Galprop*]

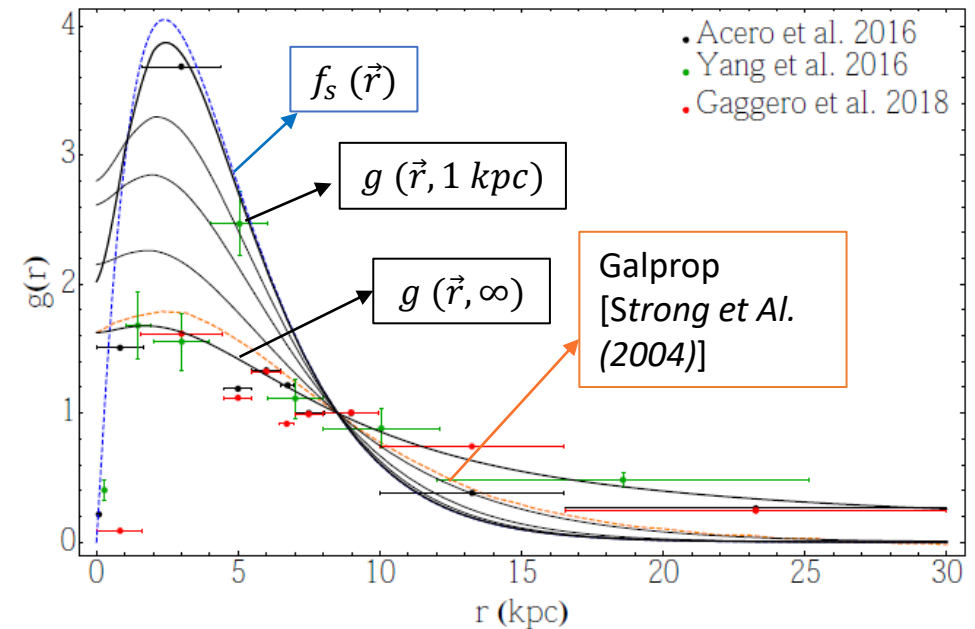
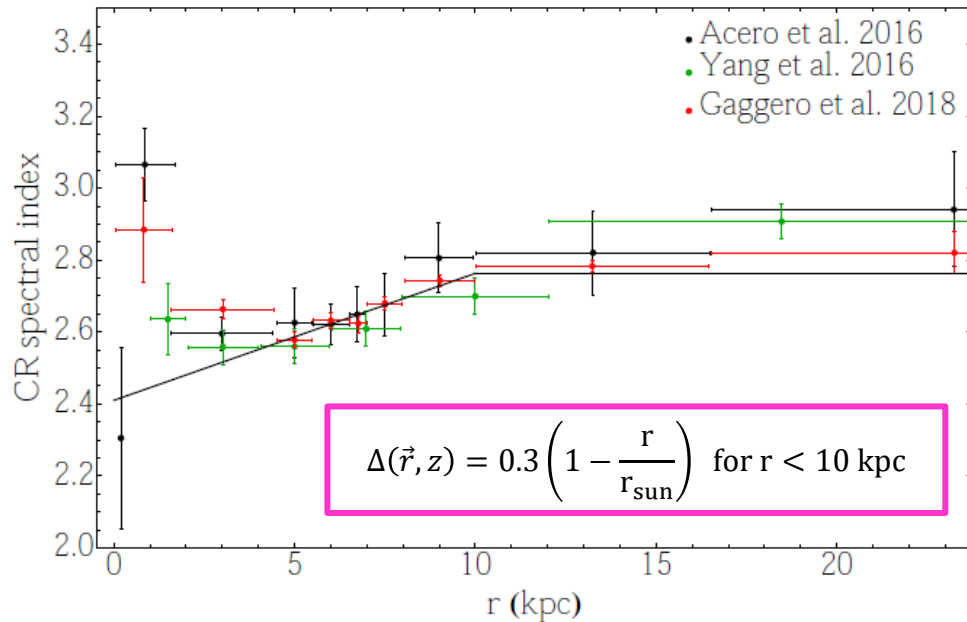
4 models for the diffuse fluxes for **4 assumptions of the CR distribution** in the Galaxy.

Cosmic ray distribution:

$$\varphi_{CR}(E, \vec{r}) = \varphi_{CR, Sun}(E) g(\vec{r}, R) h(E, \vec{r})$$

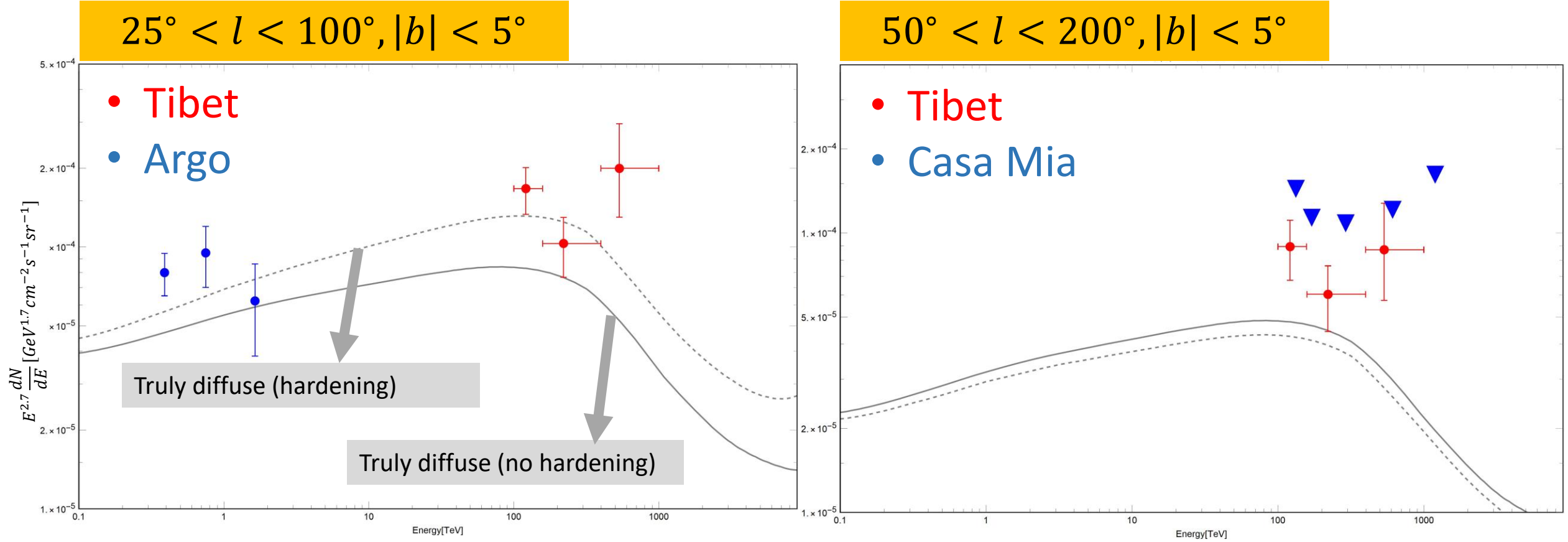
- ★ Data driven local CR spectrum [*Dembinski, Engel, Fedynitch et al. (2018)*]
- ★ $g(r)$ is determined by the distribution of the CR sources $f_s(\vec{r})$ (proportional to the SNR number density by Green et al. (2015), and by the propagation of CR in the Galactic magnetic field.
- ★ **2 cases: with and without spatially dependent CR spectral index** (from the analysis of the FermiLAT data at ~ 20 GeV [*Acero et al. (2016)*, *Yang et al. (2016)*, *Gaggero et al. (2018)*])

$$h(E, \vec{r}) = \left(\frac{E}{20 \text{ GeV}} \right)^{\Delta(\vec{r})}$$



Diffuse Galactic gamma-ray emission:

Definition: Hardening \equiv spatially dependent CR spectral index



Similar results are obtained using the models described in Lipari & Vernetto, Phys. Rev. D (2018)

Unresolved Source component:

We have $\Phi_{1-100 \text{ TeV}} \rightarrow$ we need $\phi(E)$:

- Spectral assumption: power-law with an exponential cut-off.

$$\varphi(E) = \left(\frac{E}{1 \text{ TeV}} \right)^{-\beta_{\text{TeV}}} \text{Exp} \left(-\frac{E}{E_{\text{cut}}} \right)$$

$\beta_{\text{TeV}} = 2.3$ from the HGPS catalogue;

Unresolved Source component:

We have $\Phi_{1-100 \text{ TeV}} \rightarrow$ we need $\phi(E)$:

- Spectral assumption: power-law with an exponential cut-off.

$$\varphi(E) = \left(\frac{E}{1 \text{ TeV}} \right)^{-\beta_{\text{TeV}}} \text{Exp} \left(-\frac{E}{E_{\text{cut}}} \right)$$

$\beta_{\text{TeV}} = 2.3$ from the HGPS catalogue;

$E_{\text{cut}} = 500 \text{ TeV}$ still not well constrained but motivated by recent observations of Tibet, HAWC and LHAASO;

Amenomori, M., Bao, Y. W., Bi, X. J., et al. 2019, Phys.323Rev. Lett., 123, 051101

Abeysekara, A., Albert, A., Alfaro, R., et al. 2020, Physical316Review Letters, 124

Cao, Z., Aharonian, F. A., An, Q., et al. 2021, Nature, 594,33033

Unresolved Source component:

We have $\Phi_{1-100 \text{ TeV}} \rightarrow$ we need $\phi(E)$:

- Spectral assumption: power-law with an exponential cut-off.

$$\phi(E) = \left(\frac{E}{1 \text{ TeV}} \right)^{-\beta_{\text{TeV}}} \text{Exp} \left(-\frac{E}{E_{\text{cut}}} \right)$$

$\beta_{\text{TeV}} = 2.3$ from the HGPS catalogue;

$E_{\text{cut}} = 500 \text{ TeV}$ still not well constrained but motivated by recent observations of Tibet, HAWC and LHAASO;

Amenomori, M., Bao, Y. W., Bi, X. J., et al. 2019, Phys.323Rev. Lett., 123, 051101

Abeysekara, A., Albert, A., Alfaro, R., et al. 2020, Physical316Review Letters, 124

Cao, Z., Aharonian, F. A., An, Q., et al. 2021, Nature, 594,33033

We introduce a flux detection threshold based on the performance of H.E.S.S.

$$\phi_{th} = 0.01\phi_{crab} - 0.1\phi_{crab}$$



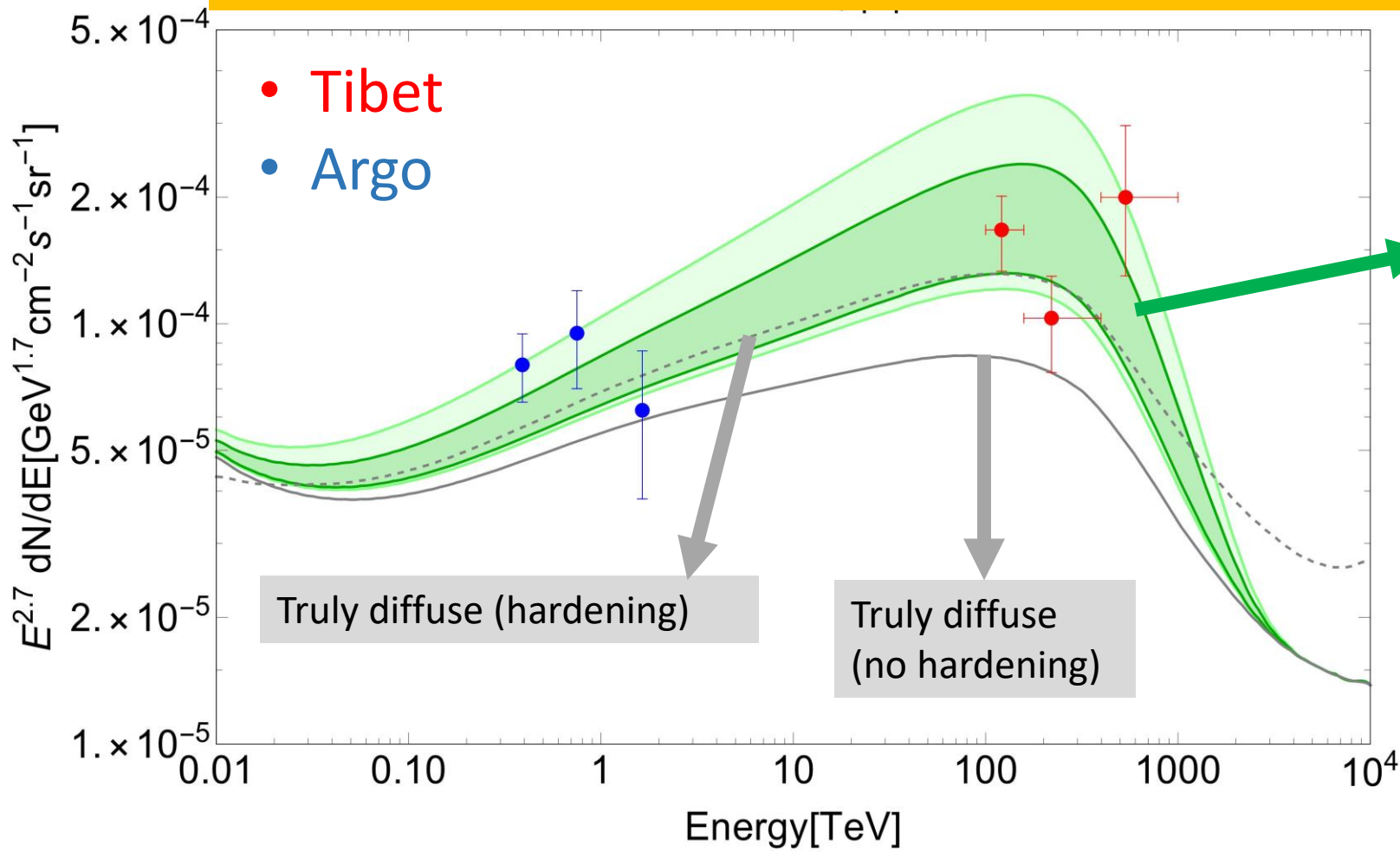
We calculate the unresolved source contribution.

Tibet $AS\gamma$: We add the contribution of unresolved sources to the truly diffuse emission without the hypothesis of CR spectral hardening.

Tibet $AS\gamma$: We add the contribution of unresolved sources to the truly diffuse emission without the hypothesis of CR spectral hardening.

Definition: Hardening \equiv spatially dependent CR spectral index

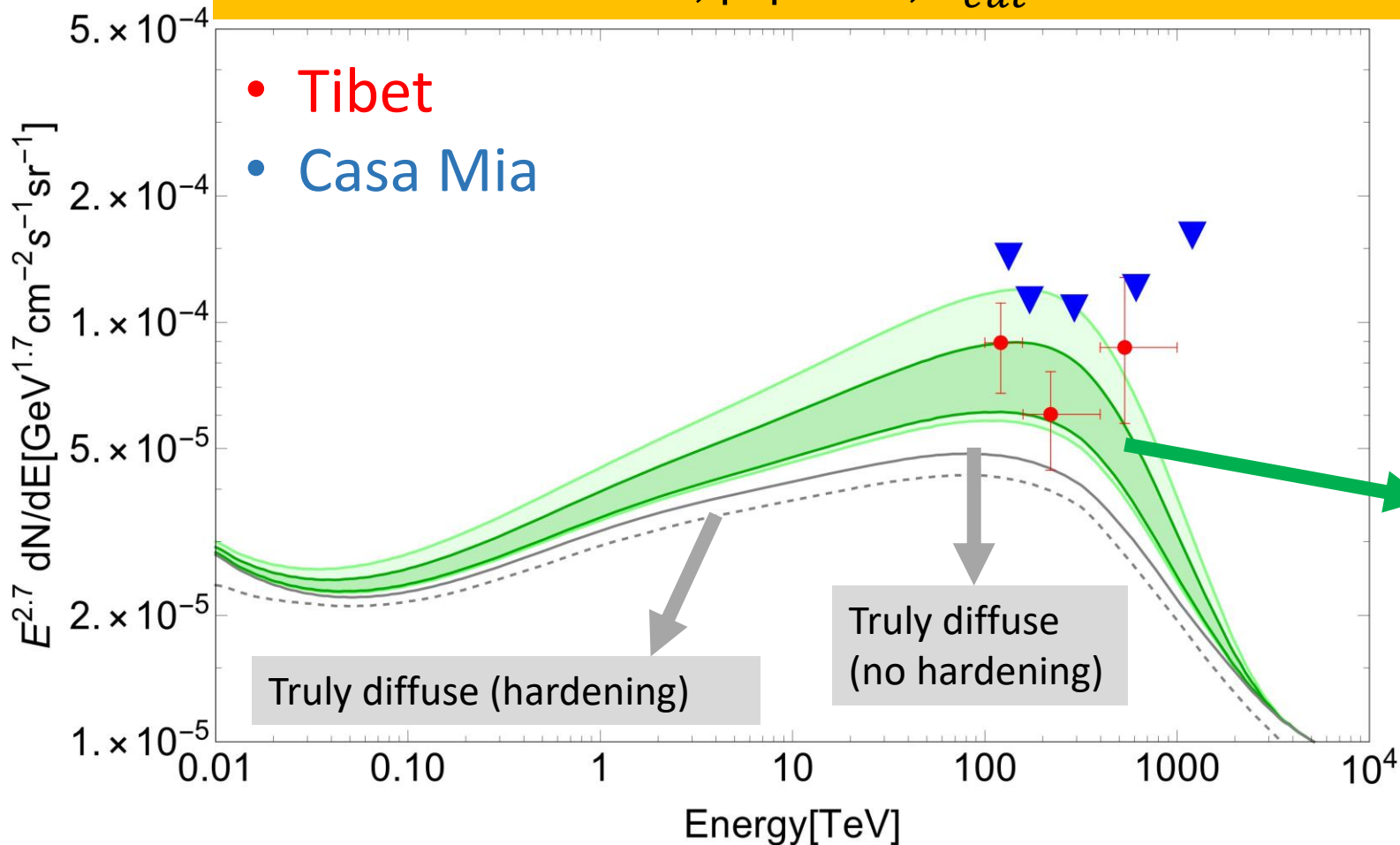
$25^\circ < l < 100^\circ, |b| < 5^\circ, E_{cut} = 500 \text{ TeV}$



Tibet AS γ : We add the contribution of unresolved sources to the truly diffuse emission without the hypothesis of CR spectral hardening.

Definition: Hardening \equiv spatially dependent CR spectral index

$50^\circ < l < 200^\circ, |b| < 5^\circ, E_{cut} = 500 \text{ TeV}$

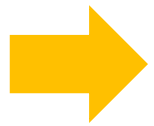


Luminosity index: $\alpha = 1.5$

Unresolved sources +
Truly diffuse (no hardening)

Take home message:

- In the **PeV** energy range the inclusion of the **unresolved PWNe** contribution produces a better description of the Tibet data than CR spectral hardening;



Looking at different sky regions is fundamental because it allows us to distinguish between the two effects.



Conclusions and outlook:

- The diffuse gamma-ray and neutrino emission can provide important information about CR spatial and energy distribution in the Galaxy. However, it is important to properly take into account the contribution of unresolved sources.
- We performed a population study of the HGPS catalog in order to infer the general properties of TeV sources (e.g. to determine their luminosity distribution, the total luminosity, the total flux, etc) and to estimate the unresolved source component.
- The contribution of unresolved sources is not negligible and it is about $\sim 40\%$ of the resolved signal measured by H.E.S.S.;

Conclusions and outlook:

- We show that a non-negligible fraction of TeV PWNe cannot be resolved by Fermi-LAT;
- We performed a Galactocentric ring analysis of the measured large-scale diffuse emission including the contribution of both unresolved TeV PWNe and the hadronic diffuse emission;
- We show that the inclusion of unresolved TeV PWNe could account for a part of the spectral index variation observed by Fermi-LAT, in particular in the inner Galaxy;

Conclusions and outlook:

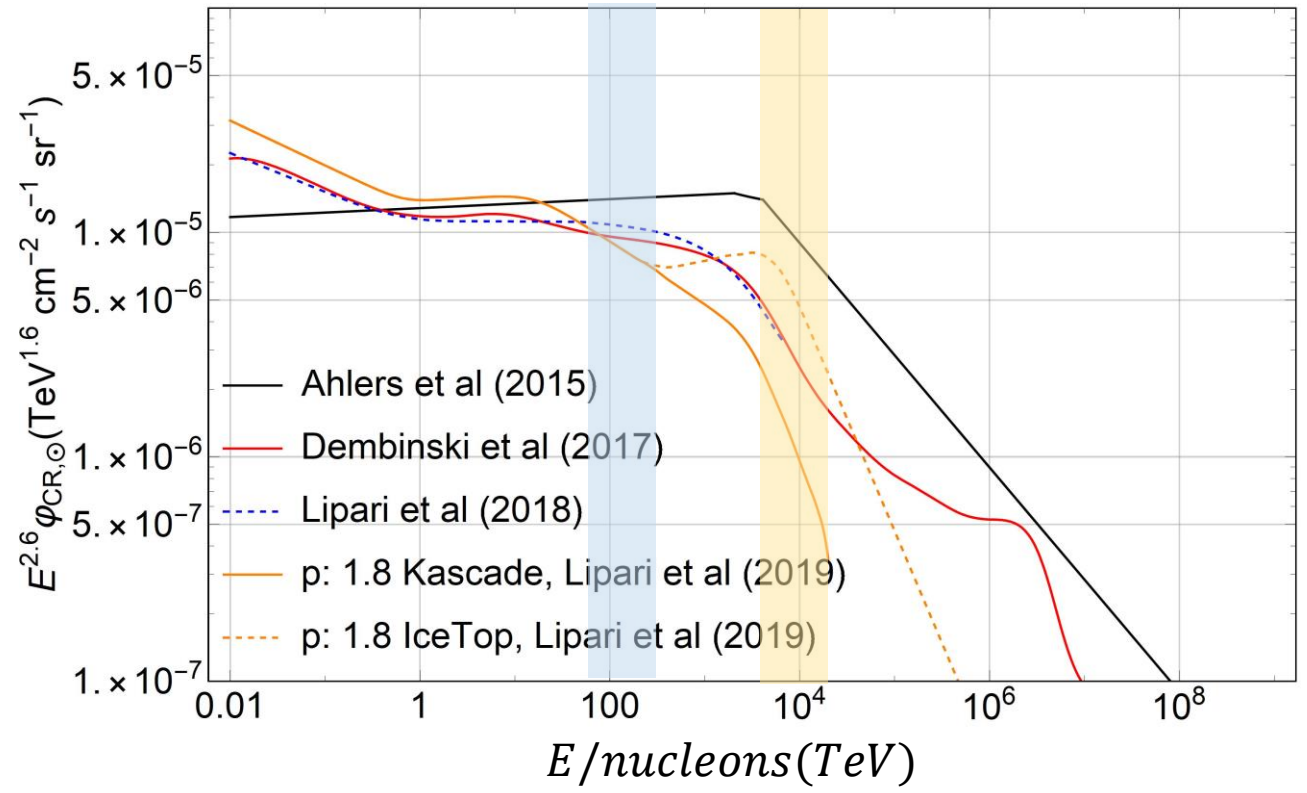
- We show that a non-negligible fraction of TeV PWNe cannot be resolved by Fermi-LAT;
- We performed a Galactocentric ring analysis of the measured large-scale diffuse emission including the contribution of both unresolved TeV PWNe and the hadronic diffuse emission;
- We show that the inclusion of unresolved TeV PWNe could account for a part of the spectral index variation observed by Fermi-LAT, in particular in the inner Galaxy;

- We calculate the unresolved component in the sub-PeV energy range using our knowledge of the TeV source population.
- We add the contribution of unresolved sources to the truly diffuse emission without the hypothesis of CR spectral hardening;
- In the sub-PeV energy range the inclusion of the unresolved PWNe contribution produces a better description of the Tibet data than CR spectral hardening;

Backup slides

Cosmic ray distribution:

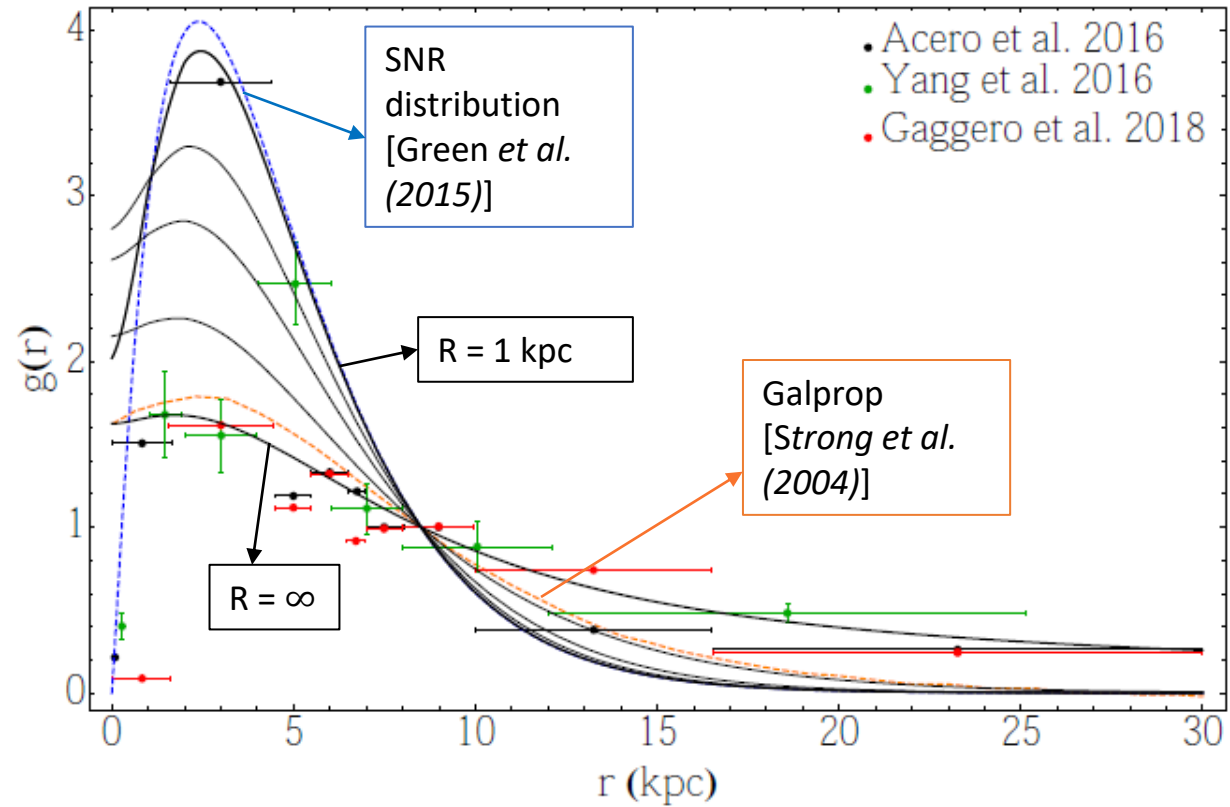
$$\varphi_{CR}(E, \vec{r}) = \varphi_{CR, Sun}(E) g(\vec{r}, R) h(E, \vec{r})$$



- Data driven local CR spectrum;
Dembinski, Engel, Fedynitch et al. (2018)
- The gamma-ray (neutrino) flux at $E_\gamma = 1 TeV$ ($E_\nu = 100 TeV$) is determined by CRs with $E_{CR} = 10 TeV$ ($E_{CR} = 2 PeV$);

Cosmic ray distribution:

$$\varphi_{CR}(E, \vec{r}) = \varphi_{CR, Sun}(E) g(\vec{r}, R) h(E, \vec{r})$$



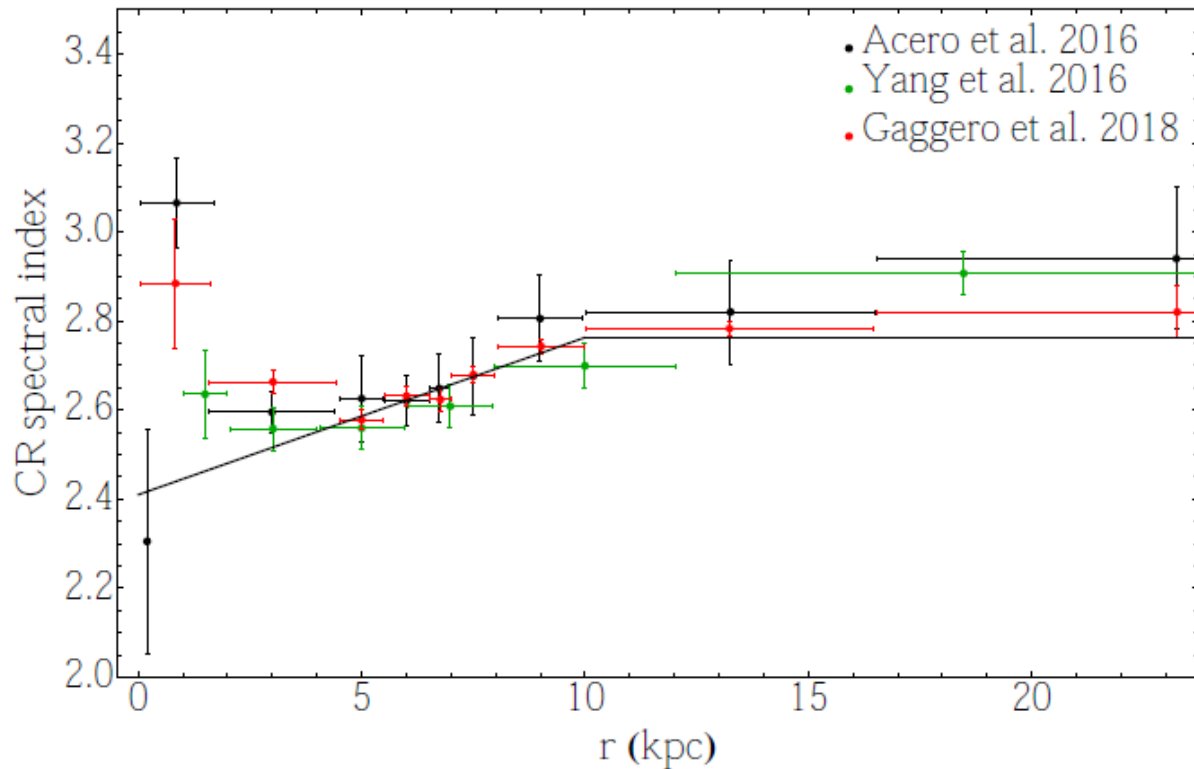
- Data driven local CR spectrum; *Dembinski, Engel, Fedynitch et al. (2018)*
- The function $g(r)$ is determined by the distribution of the CR sources $f_s(\vec{r})$ and by the propagation of CR in the Galaxy;

$$g(\vec{r}) = \frac{1}{N} \int d^3x \frac{f_s(\vec{r} - \vec{x}) F\left(\frac{|\vec{x}|}{R}\right)}{|\vec{x}|}$$

$$F(v) = \frac{1}{\sqrt{2\pi}} \int_v^\infty d\gamma \exp(-\gamma^2/2)$$

Cosmic ray distribution:

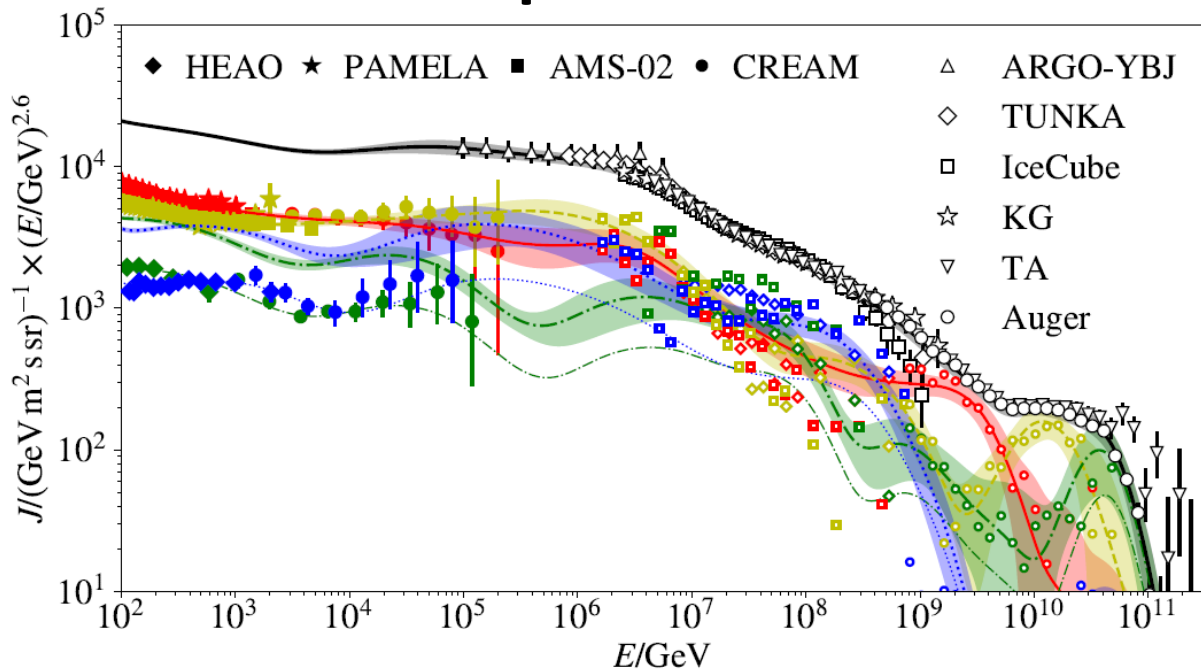
$$\varphi_{CR}(E, \vec{r}) = \varphi_{CR, Sun}(E) g(\vec{r}, R) h(E, \vec{r})$$



$$h(E, \vec{r}) = \left(\frac{E}{20 \text{ GeV}}\right)^{\Delta(\vec{r})}; \Delta(\vec{r}) = 0.3 \left(1 - \frac{r}{r_{\text{sun}}}\right) \text{ for } r < 10 \text{ kpc}$$

- Data driven local CR spectrum;
Dembinski, Engel, Fedynitch et al. (2018)
- The function $g(r)$ is determined by the distribution of the CR sources $f_s(\vec{r})$ and by the propagation of CR in the Galaxy;
- We consider the possibility of spatially dependent CR spectral index recently emerged from the analysis of the FermiLAT data at $\sim 20 \text{ GeV}$
Acero et al. (2016), Yang et al. (2016), Gaggero et al. (2018)

CR local spectrum



At energies of few PeV, the CR spectrum is affected by large uncertainties:

- It is a transition region between different detection techniques;
- Transition from Galactic to extragalactic CRs.
- CRs compositions;

The diffuse emission is determined by the total nucleon flux that depends on the CR composition.

$$\varphi_{CR,Sun}(E) = \sum_A A^2 \frac{d\phi_A}{dE_A d\Omega_A}(AE)$$

CR nucleons spectrum

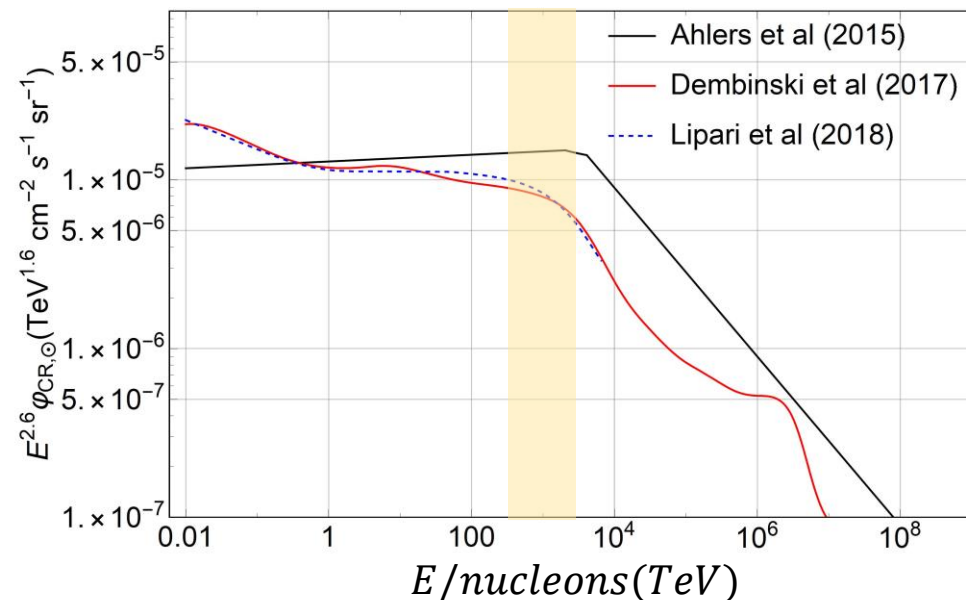


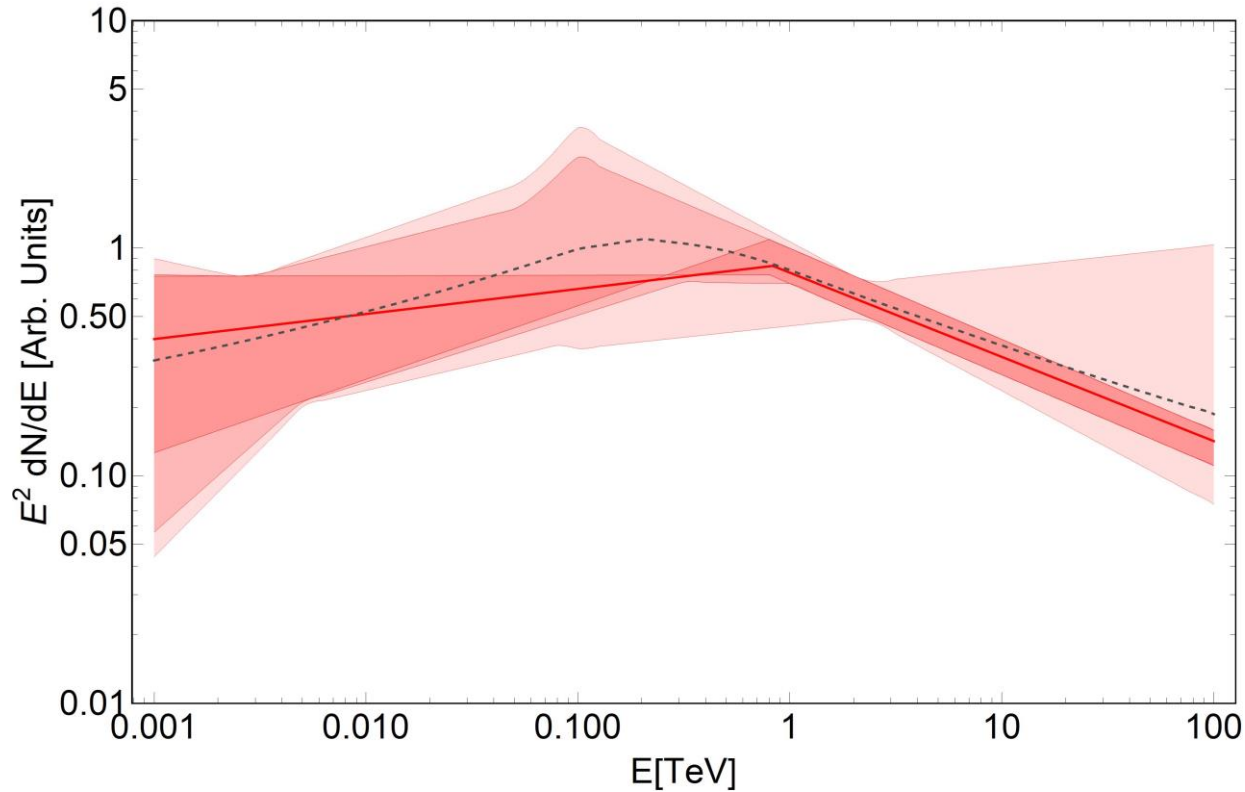
Table of the 12 sources observed by both Fermi and HESS:

Table 1: *In the table are shown the 12 PWNe observed by both FermiLAT (4FGL-DR2) and H.E.S.S. (HGPS). In addition we show also the Crab although it is not observed by H.E.S.S.. In the first columns is reported the calculated value of R_ϕ . In the second one the power-law spectral index (it is specified when the spectral form is different than a simple power-law) in the GeV energy range taken from the 4FGL-DR2 catalogue. In the last column is reported the power-law spectral index (it is specified when the spectral form is different than a simple power-law) in the TeV energy range taken from the HGPS catalogue.*

H.E.S.S.-association	R_ϕ	β_{GeV}	β_{TeV}	D(kpc)	τ_c (kyr)
Crab	1481.24	1.38 (1 GeV) (log-par)	2.30	2.0	0.94
HESS J0835-455	754.938	2.18	1.89	0.29	11.3
HESS J1303-631	447.05	1.81	2.33	6.7	11.0
HESS J1356-645	63.47	1.41	2.20	2.4	7.31
HESS J1420-607	999.354	1.99	2.20	5.6	13.0
HESS J1616-508	1223.36	2.05	2.32	6.8	8.13
HESS J1632-478	799.56	1.76	2.51	-	-
HESS J1746-285	98950.	0.96 (1 GeV) (log-par)	2.17	-	-
HESS J1825-137	582.721	1.73	2.38	3.9	21.4
HESS J1837-069	1612.13 (483.598)	2.04 (1.84)	2.54	6.6	22.7
HESS J1841-055	1149.91	1.98	2.47	-	-
HESS J1857+026	2390.84	2.12	2.57	-	20.6
HESS J1514-591	686.30	1.83	2.05	5.2	1.56



Effects of parameter space:



The unresolved source flux is either large or has a hard spectrum:

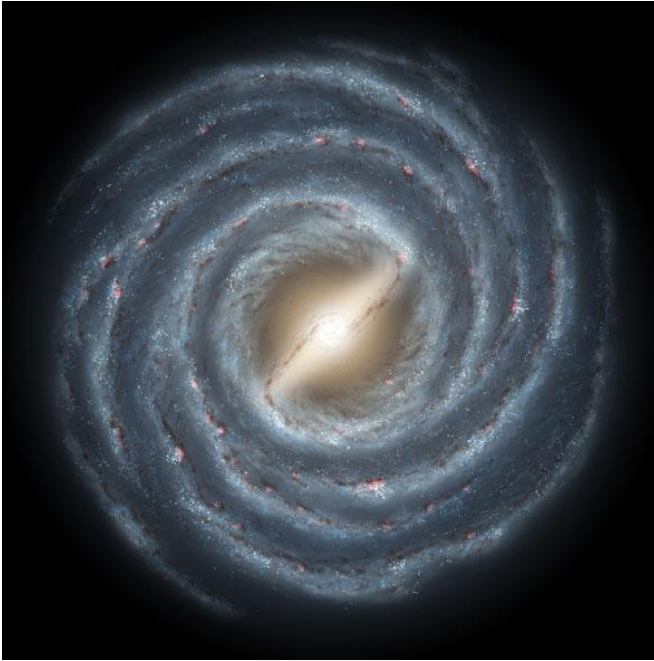
$$R_\phi = 250 (E_0 = 0.8 \text{ TeV}, \beta_{TeV} = 2.4) \rightarrow \beta_{GeV} = 1.67$$

$$R_\phi = 1500 (E_0 = 0.8 \text{ TeV}, \beta_{TeV} = 2.4) \rightarrow \beta_{GeV} \sim 2$$

This behavior is because the flux in the TeV energy range is fixed (constrained by the population study of the H.G.P.S catalog).

The unresolved flux is affected by large uncertainties at few GeV that become smaller as the energy increase because of the constraint in the TeV energy range

PWNe contribution in galactocentric rings



	$\Phi_{\text{GeV}}^{\text{diff}} (cm^{-2} s^{-1})$	$\Phi_{\text{GeV}}^{\text{NR}} (cm^{-2} s^{-1})$		$\Phi_{\text{GeV}}^{\text{NR}} (cm^{-2} s^{-1})$	
		$R_{\Phi} = 250, \alpha = 1.8$	$R_{\Phi} = 1500, \alpha = 1.8$	$R_{\Phi} = 250, \alpha = 1.5$	$R_{\Phi} = 1500, \alpha = 1.5$
1.7 – 4.5 kpc	3.86×10^{-7}	3.35×10^{-8} (8.6%)	1.40×10^{-7} (36%)	1.60×10^{-8} (4.1%)	3.92×10^{-8} (10%)
4.5 – 5.5 kpc	3.11×10^{-7}	1.91×10^{-8} (6.1%)	8.00×10^{-8} (26%)	8.30×10^{-9} (2.7%)	2.00×10^{-8} (6.4%)
5.5 – 6.5 kpc	5.09×10^{-7}	2.13×10^{-8} (4.2%)	8.93×10^{-8} (17%)	8.33×10^{-9} (1.6%)	2.02×10^{-8} (3.9%)
6.5 – 7.0 kpc	2.57×10^{-7}	1.15×10^{-8} (4.5%)	4.81×10^{-8} (19%)	3.96×10^{-9} (1.5%)	9.48×10^{-9} (3.7%)
7.0 – 8.0 kpc	7.7×10^{-7}	2.67×10^{-8} (3.5%)	1.12×10^{-7} (14%)	7.53×10^{-9} (1.0%)	1.83×10^{-8} (2.4%)
8.0 – 10.0 kpc	3.84×10^{-6}	4.89×10^{-8} (1.3%)	2.05×10^{-7} (5.3%)	1.08×10^{-8} (0.3%)	2.69×10^{-8} (0.7%)
10.0 – 16.5 kpc	7.68×10^{-7}	1.51×10^{-8} (1.9%)	6.37×10^{-8} (8.3%)	6.37×10^{-9} (0.8%)	1.65×10^{-8} (2.1%)
16.5 – 50.0 kpc	4.44×10^{-8}	3.87×10^{-10} (0.8%)	2.07×10^{-9} (4.7%)	2.43×10^{-10} (0.5%)	6.98×10^{-10} (1.6%)
0.0 – 50.0 kpc	6.89×10^{-6}	1.79×10^{-7} (2.6%)	7.53×10^{-7} (11%)	6.28×10^{-8} (1.0%)	1.54×10^{-7} (2.2%)

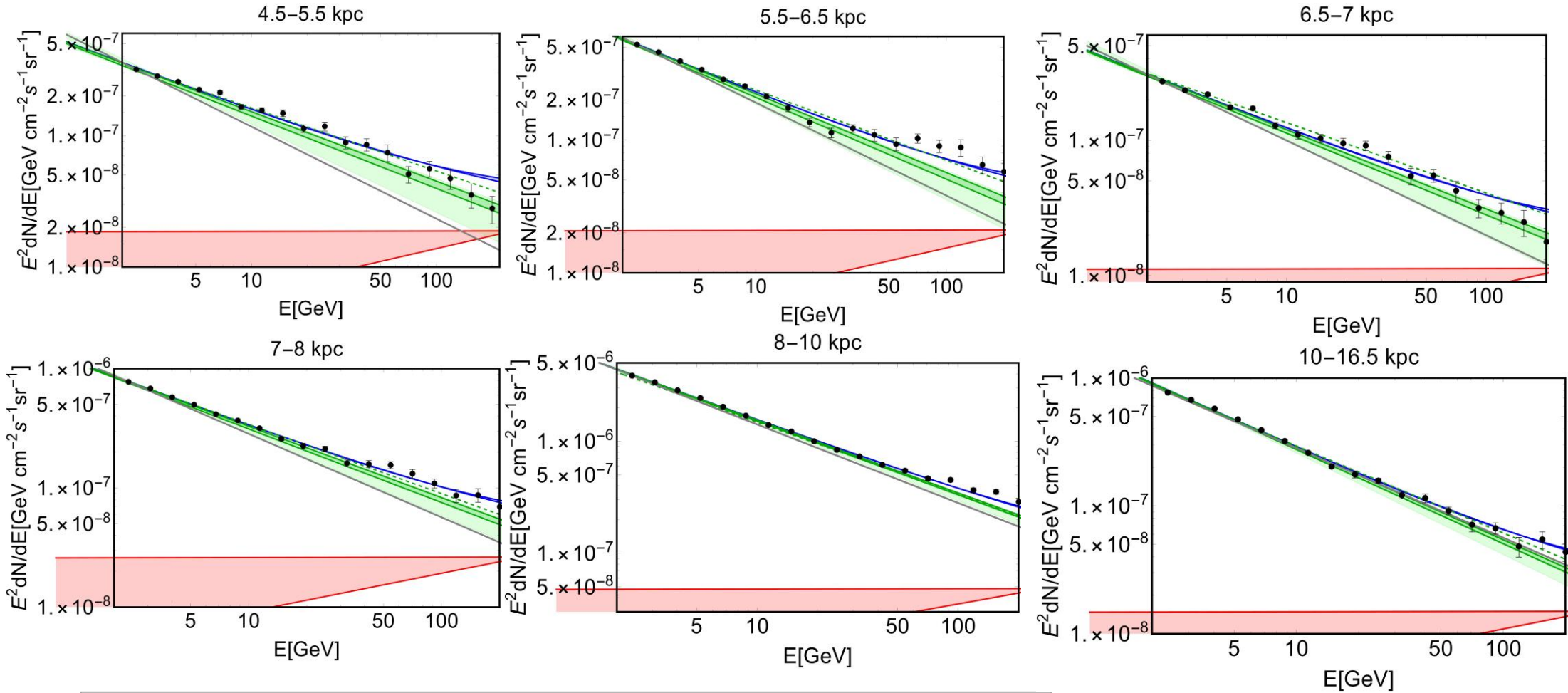
9 Galactocentric rings

Total diffuse emission: 9.3 years of Fermi-LAT Pass 8 data (0.34–228.65) GeV and ($|\ell| < 180^\circ$) and $|b| < 20.25^\circ$

Diffuse emission due to unresolved PWNe (1-100) GeV with $\alpha = 1.8$

Diffuse emission due to unresolved PWNe (1-100) GeV with $\alpha = 1.5$

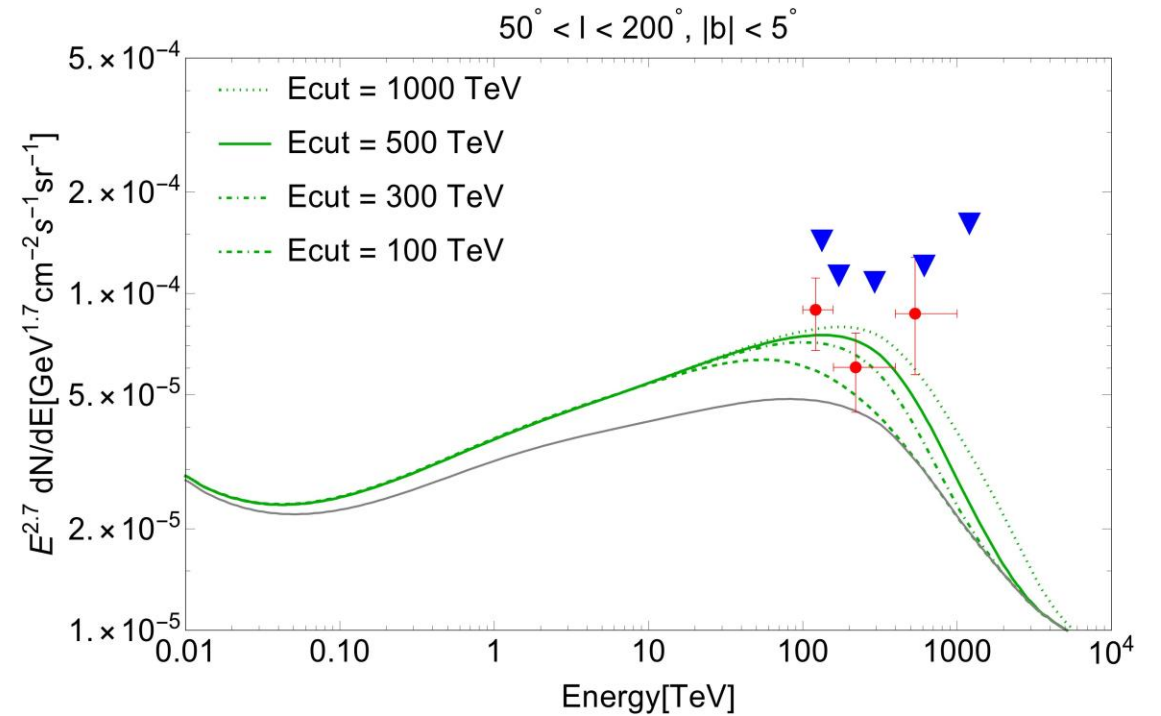
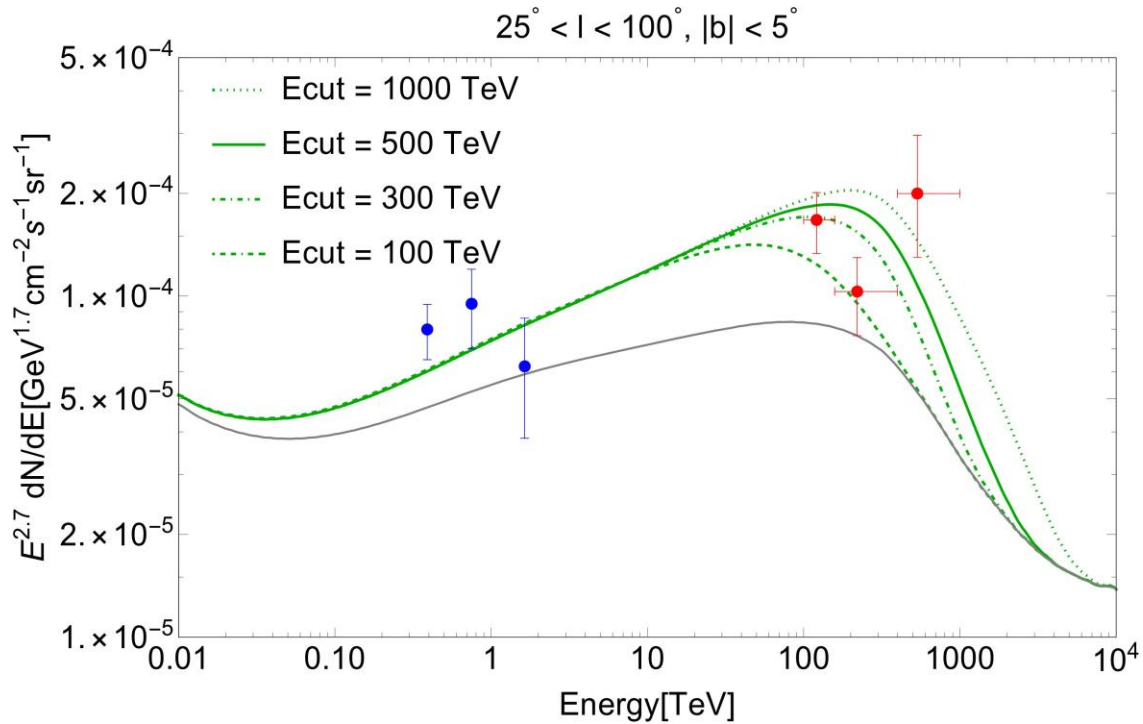
Results for $\alpha = 1.8$



Gray line: speculative diffuse component with spectral index fixed to 2.7 normalized in order to interpolate the data at ~ 2 GeV.

Cut-off effect:

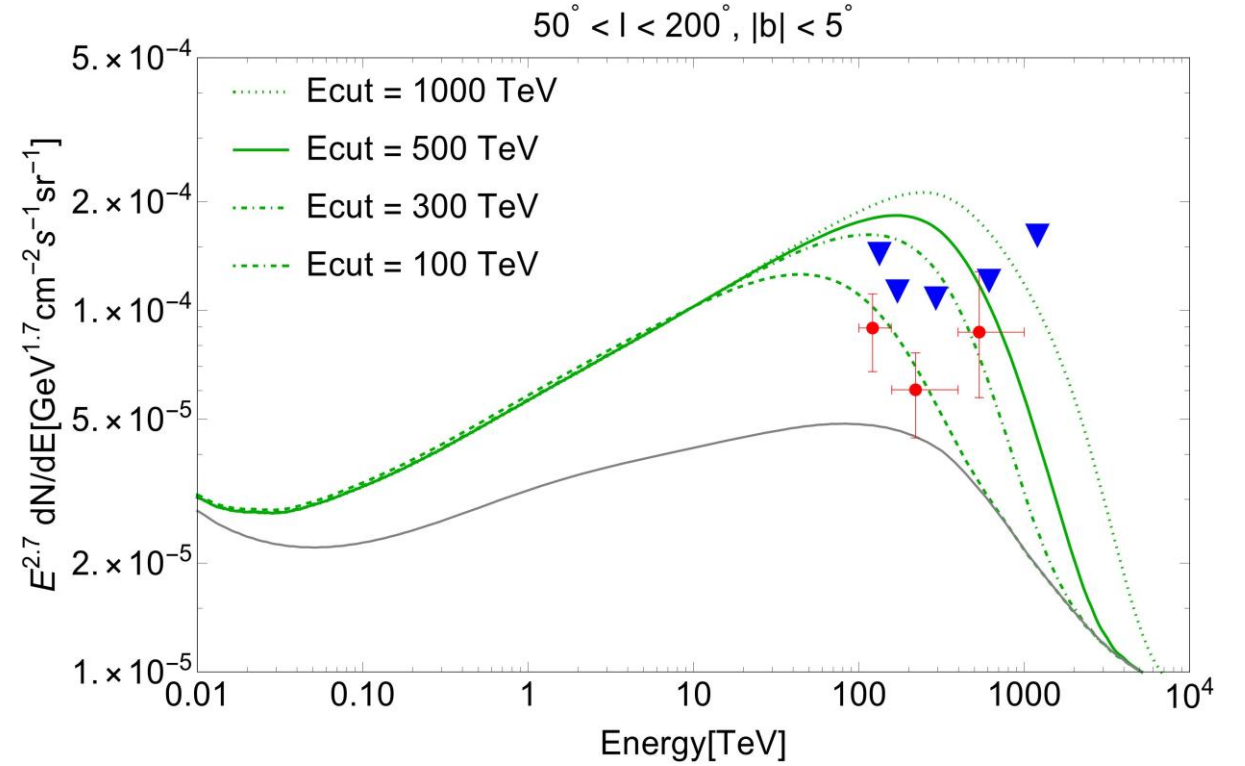
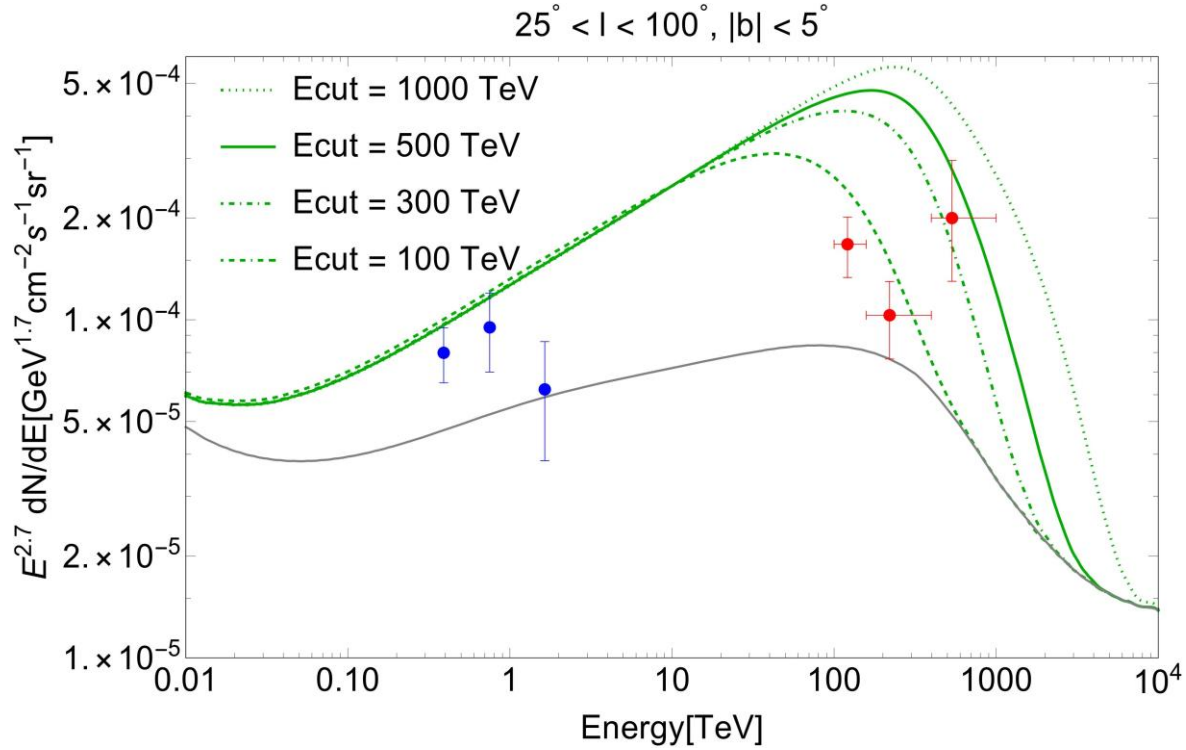
Luminosity index: $\alpha = 1.5$



- The green lines are calculated assuming an intermediate threshold: $\phi_{th} = 0.5\phi_{crab}$
- The capability to explain the first two data-points does not depend on the assumed cut-off;
- The third data point is out in case of $E_{cut} < 500$ TeV

Cut-off effect:

Luminosity index: $\alpha = 1.8$



Tibet AS γ : Cut-off fixed to 100 TeV:

Luminosity index: $\alpha = 1.8$

